CHAPTER 8

Photocatalytic Treatment of Air: From Basic Aspects to Reactors

Yaron Paz

Contents

Department of Chemical Engineering, Technion-Israel Institute of Technology, Haifa, Israel.
E-mail address: paz@tx.technion.ac.il

Advances in Chemical Engineering, Volume 36
ISSN 0065-2377, DOI: 10.1016/S0065-2377(09)00408-6

1. INTRODUCTION

The growing awareness to our environment and to the conditions of living brings along an increasing scientific and commercial tendency to develop new, effective, and inexpensive means to improve the quality of water and air. Advanced oxidation processes (AOP) and in particular TiO_2 photocatalysis are now considered as true competitors to the classical techniques of purification. Accordingly, an increasing number of scientific manuscripts and patents can be found in the literature.

If one looks at the way photocatalysis has developed over the years, one finds out that the first applications to be considered following the pioneering paper of Fujishima and Honda (1972) were related to energy, that is, to water splitting, (Cunningham et al., 1981; Pelizzetti et al., 1981) as energy is something we all pay for, something whose shortage can be foreseen within, historicallywise, a very short time. It took awhile until the possibility of using the photocatalytic properties of titanium dioxide for environmental purposes was realized. From the chronicle point of view, the interest in water purification began prior to air treatment. In fact, this seniority, in terms of the number of scientific manuscripts, is still kept until these days. A quantified view of these statements is presented in Figure 1, which

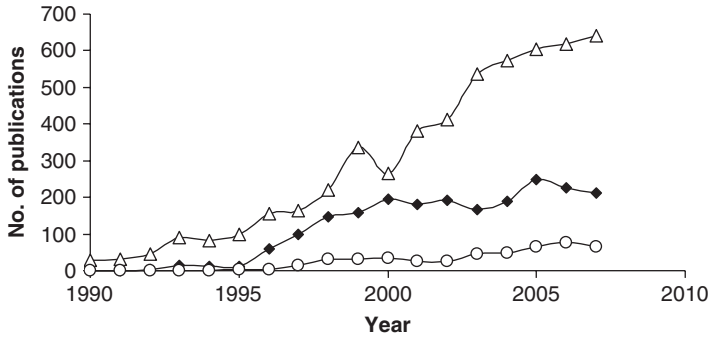

Figure 1 Estimated number of scientific manuscripts on titanium dioxide photocatalysis per year, categorized according to water treatment (empty triangles), air treatment (filled diamonds), self-cleaning surfaces (empty circles).

presents the estimated number of scientific manuscripts on titanium dioxide photocatalysis per year, categorized according to water treatment, air treatment, and self-cleaning surfaces.

The results presented in Figure 1 were acquired by counting hits upon using SciFinder Scholar™ (2007) as our search engine, having "titanium dioxide," "photocatalysis," and "air treatment/water treatment/self-cleaning" as keywords. It is obvious that the total number of publications on titanium dioxide photocatalysis is larger than the sum of papers in these three categories, as these cannot cover all the publications in the field, while the percentage of publications, which belong to more than one category, is (according to our impression) quite low. It is likely that other search engines might give different number of hits. It is further likely that a few of the relevant publications did not mention explicitly the medium in their abstracts. Yet, regardless of the exact numbers, it is reasonable to believe that the main features of the graphs, namely, the lag in the research on air treatment, the monotonically increase in the number of publications in each of the categories, and the fact that water treatment is still the subject of most of the TiO_2 photocatalysis manuscripts are genuine.

There could be several reasons for this situation: the common feeling that air (despite being essential for life) is not regarded as something that one (whether be a politician or the average person in the street) has to pay for, unlike water whose price is familiar to all (including grants agencies), in particular in the arid countries. It is also possible, that the fact that the first group of researchers came from the electrochemistry community played a role here. Anyway, whatever the reasons are, the higher number of publications on water treatment relative to air treatment cannot be denied. Interestingly enough, it seems that the scientific community was aware of this fact quite a few years ago (Alberici and Jardim, 1997). Nevertheless, it also seems that the scientific community was much less aware to the growing interest of the industrial and the commercial community, manifested, for example, by the number of patents in air – treatment.

Figure 2 presents the annual number of new patents on titanium dioxide photocatalysis categorized according to the three categories of Figure 1. From the figure, it is evident that the year 1995 was a turning point year with respect to the number of issued patents. The years 1995–2000 seem to be the "booming" years in which the annual number of patents grew fast and monotonically. Ever since year 2000, the annual number of patents remained constant more or less, probably indicating that the field enters its maturity period. The fact that as of 1997 the number of patents on air treatment surpasses that of water treatment is quite striking, especially if one takes into account that the number of scientific publications on water treatment is larger than that of air treatment (Figure 1).

The large annual number of patents on photocatalytic air treatment is portrayed again in Figure 3, which presents the distribution of patents

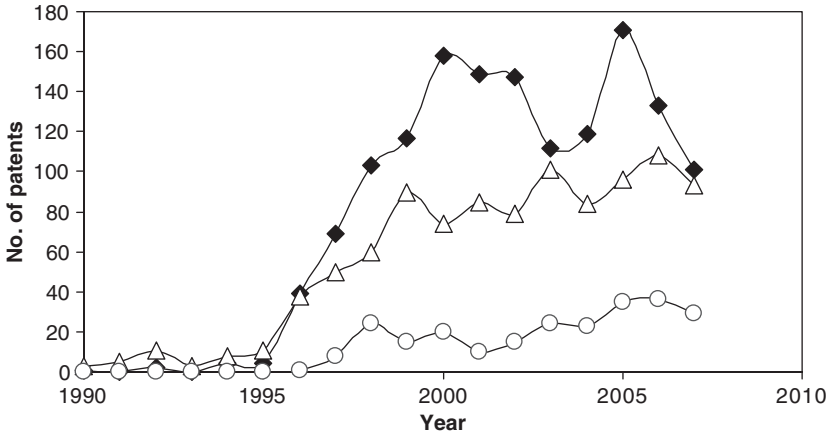

Figure 2 Estimated number of patents on titanium dioxide photocatalysis per year, categorized according to water treatment (empty triangles), air treatment (filled diamonds), self-cleaning surfaces (empty circles).

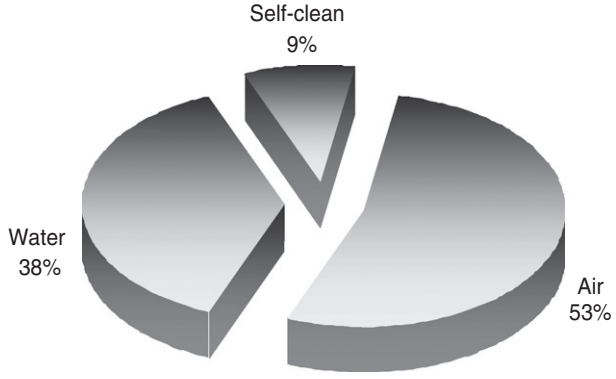

Figure 3 The distribution of patents between the three major categories (air treatment, water treatment, self-cleaning) on a cumulative basis.

between the above-mentioned three categories on a cumulative basis. Evidently, the number of patents on air treatment is larger than the sum of patents on water treatment and on self-cleaning surfaces. The fact that there are more patents on photocatalytic air treatment compared with the other two categories is not obvious, especially if one considers the fact that cleaned surfaces are in demand in the market, being tangible products that people are willing to pay for, and likewise are water, whose economical value is clear to anyone, even for those who do not use the so-called shadow cost of water.

This chapter tries to analyze the use of titanium dioxide for photocatalytic air treatment. For this, the various types of applications will be discussed, as well as the mechanisms and reaction kinetics of some of the most popular model contaminants. Care will be given to characterize the large variety of photocatalytic reactors in use for air treatment.

2. TYPES OF AIR-TREATMENT APPLICATIONS

In the context of gas-phase photocatalysis, it is possible to identify four major types of applications: indoor, outdoor, process gases, and dissolved pollutants. These four types have characteristic properties, which may (in certain cases may not) affect the effectiveness of photocatalysis relative to other means of treatment and the type of optimal photoreactor and material to be used.

Figure 4 presents the annual number of manuscripts dedicated to photocatalytic indoor air treatment as well as the annual number of papers dedicated to photocatalytic outdoor treatment, as deduced from the number of SciFinder Scholar hits. Here, there was no point in trying to get information on the other two types, as the terms "process gases" and "dissolved pollutants" (or any other terms) are not associated strongly enough and specifically enough with these types of applications, hence the error, if such an attitude would have been taken, could have been quite large. The figure clearly demonstrates that the scientific interest in photocatalytic indoor air treatment is by far larger than that of photocatalytic outdoor air treatment.

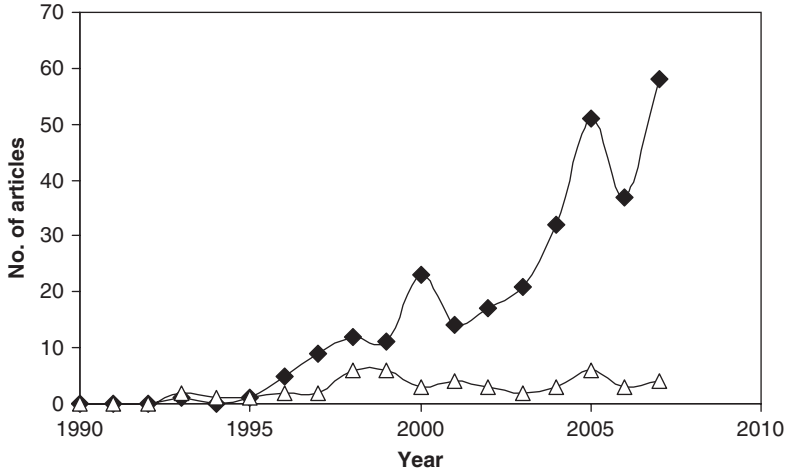

Figure 4 Estimated number of manuscripts per year on photocatalytic indoor air treatment (filled diamonds) and on photocatalytic outdoor air treatment (empty triangles).

Furthermore, the number of manuscripts on photocatalytic indoor air treatment seems to grow very fast over the last decade, in correlation with the trend of the overall number of manuscripts on photocatalytic air treatment (Figure 1).

2.1. Indoor air treatment

The modern human being lives in an urban environment and spends as much as 70–90% of his time indoors (Aguado et al., 2004), where ventilation, under the constrains of energy price, architecture, and lack of awareness of its importance, might be far less than optimal. The variety of chemicals emitted indoors is enormous. A simple ink-jet printer, one of so many potential sources for indoor pollutants, emits no less than 18 pollutants, among which are benzene, toluene, chloroform, methylene chloride, styrene, ozone, and many more (Lee et al., 2001). Even an innocent-looking device, such as the computer on which this manuscript is written at this moment, emits 100–200 μg of volatile organic compounds (VOCs) per hour (Destaillats et al., 2008). Investigations of gaseous contaminants in buildings, including buildings that suffer from the so-called sick building syndrome (SBS), have shown that the concentrations of individual species are as low as 0.1 parts per million by volume (ppmv) and that the total concentration of VOCs are between 0.5 and –2.0 ppmv (Obee and Brown, 1995). The indoor level of pollutants was found to be on the average higher than that at the nearby outdoor environment, indicating the importance of indoor sources (Saarela et al., 2003). No wonder that the Environmental Protection Agency considered indoor air pollution to carry a higher health risk than outdoor air pollution (EPA, 1987). It should be emphasized that within the context of this chapter, the term "indoor air," includes any confined places having levels of pollutants which are above the ambient concentrations outside of the confined place. Accordingly, the term is relevant not only to buildings but also to transportation vehicles, aircrafts, storehouses, and the like.

Photocatalysis seems to be well suited for the purification of indoor air, in particular if compared with purification of water. A very good analysis of the logics of this statement was given by Agrios and Pichat (2005) who pointed out that the low concentrations of pollutants found in air facilitates continuous operation without saturating the surface of the photocatalyst. There are also several drawbacks associated with using photocatalysis for indoor air treatment. These drawbacks are often related to the formation of by-products or end-products that block the active sites. Among the deactivating pollutants, one may mention benzene and other aromatic compounds, trichloroethylene (TCE), and, probably most important, organo-silicone compounds that become more and more in use as sealants.

2.2. Outdoor air treatment

Several researchers have claimed that roads painted with titanium dioxide or the use of buildings covered with cementitious materials containing TiO_2 may improve the quality of ambient air (Takeuchi, 1998), for example, by removing the aromatic group of compounds known as BTEX (Strini et al., 2005). Indeed, measurements under conditions that simulated canyon-type streets measured NOx concentration values that were 37–82% lower than the ones measured in the absence of TiO_2 coating (Maggos et al., 2008). Nevertheless, due to mass transport limitations (the need for the pollutants to reach the photocatalyst surface), practical use of photocatalysis for air decontamination is expected to be restricted to confined places such as canyon streets, as was justly pointed out by Agrios and Pichat (2005). It is noteworthy that canyon streets are more prone to collect pollutants, so in that sense, the photocatalytic solution may enter exactly at a point where it is needed. Also, photocatalysis can be specifically adequate for outdoor treatment of NOx, emitted at large by diesel vehicles, as the nitric acid formed during the photocatalytic oxidation can be washed away by rain.

Outdoor air treatment utilizes, in general, photocatalytic cementitious materials or sprayed photocatalytic coatings on walls, roads, and buildings. Quite often, these types of coatings are referred as "self-cleaning coatings," as photocatalytic coatings on construction materials act to prevent the adsorption of soot or dust that tend to stick to grimy surfaces. Although TiO_2-coated surfaces can serve, in principle, for the dual purpose of self-cleaning and outdoor air treatment, optimization for one type of application does not necessarily coincides with optimization for the second type of application. For example, for outdoor air treatment, a corrugated, high surface area film can do better than a smooth film, whereas for self-cleaning a smooth surface is preferred.

2.3. Process gases

Several works were aimed at treating gaseous pollutants, emitted as point sources at a defined location. This type of application is characterized by the fact that the pollutant is well defined in terms of compound and range of concentrations. For most cases, the concentration of the pollutant emitted from an industrial point source is higher than in indoor or in outdoor application, and the conditions are usually so that a true one-pass treatment is needed, unlike in indoor air treatment. Knowing the type of pollutant may assist in optimizing the design and operational conditions of the photoreactor. For example, some pollutants are photooxidized best on Degussa P-25 while other are degraded best on TiO_2 particles produced by Hombikat (Wang et al., 2002). One may even think on designing

photocatalysts with high specificity for specific pollutant, for example, by the "Adsorb and Shuttle" (A&S) approach (see below, Ghosh–Mukerji et al., 2003; Paz, 2006; Sagatelian et al., 2005) or by the imprinting method (Sharabi, submitted). Likewise, the optimal level of humidity depends, to some extent, on the type of pollutant. Hence a proper design should include means to control humidity at its pollutant-specific level. Also, if the pollutant-emitting process is not continuous, one should consider the coupling of an adsorbing-desorbing device together with a continuously operating photocatalytic system, thus continuing to photooxide the pollutants during idle times.

Examples for treatment of process gases include treating low-concentration gases emitted from pulp and paper mills such as methanol by using an annular packed bed reactor (PBR) (Stokke et al., 2006) and the photocatalytic degradation of pyridine, used widely in the synthesis of vitamins, drugs, and rubber chemicals, by a photocatalytic reactor based on zeolite-supported TiO_2 (Sampath et al., 1994). To these examples one may add also the oxidation of NOx to HNO_3 by titanium dioxide, as well as the reduction of NOx to N_2 by a photocatalytic zeolite matrix hosting less than 1% of TiO_2 (Kitano et al., 2007).

2.4. Dissolved pollutants

Photoreactors for dissolved pollutants operate by bubbling a carrier gas (usually air) through a reservoir of liquids (usually water). The pollutant-loaded gas is then passed though the photocatalytic reactor and released. Several types of reactors have been connected with this application, including PBRs and coated wall reactors.

To some extent, such photoreactors can be considered as a subtype of the process-gas photoreactors, as they are used to reduce the emission of volatile compounds formed in chemical processes into the ambient air. It should be noted that the practical use of this application is limited by volatility of the liquid-phase pollutants, so it is inadequate for low vapor pressure pollutants.

3. BASIC ASPECTS OF PHOTOCATALYSIS FOR AIR TREATMENT

As mentioned before, the photocatalytic process was studied extensively for water treatment, air treatment, self-cleaning of surfaces, as well as in the context of medical applications and energy conversion. Throughout the years many insights on the fundamentals of photocatalysis were obtained. Some of the insights, closely related to air treatment, are summarized briefly hereby.

3.1. Reaction kinetics

There is an intensive literature showing that in the absence of mass transfer limitations, many photocatalytic reactions follow the Langmuir–Hinshelwood (LH) kinetics described in Equation (1) for a one-component system:

$$(-r_A) \equiv -\frac{dC_A}{dt} = k_{r,A}\vartheta_A = \frac{k_{r,A}K_AC_A}{1+K_AC_A} \tag{1}$$

Here, C_A is the concentration of pollutant, t is the time, $k_{r,A}$ is the reaction rate constant, K_A is the adsorption coefficient of A, and θ_A is the surface coverage of this specie. Gas-phase examples include the degradation of toluene (Bouzaza and Laplanche, 2002), methyl tert-butyl-ether (Boulamanti and Philippopoulos, 2008), dimethylamine (Kachina et al., 2007), ethanol (Vorontsov and Dubovitskaya, 2004), and other VOCs (Mills and Le Hunte, 1997). When K_AC_A is small, this equation is degenerated into a typical first-order expression, where k_{app} the apparent first-order constant is approximately $k_{r,A}K_A$. Since the apparent rate constant depends on both $k_{r,A}$ and K_A, a lower adsorption constant does not always result in a lower degradation rate, as demonstrated by Bouzaza et al. (2006).

It is noteworthy that observation of LH kinetics does not necessarily imply a surface reaction (Turchi and Ollis, 1990), although in most cases this may be correct. In addition, one should not overlook a possible contribution from oxidizing species that leave the photocatalyst surface and operate by the so-called remote degradation effect (Haick and Paz, 2001; Lee and Choi, 2002; Murakami et al., 2007; Tatsuma et al., 2001; Zemel et al., 2002).

Presenting Equation (1) in its reciprocal form,

$$\frac{1}{(-r_A)} = \frac{1}{k_{r,A}} + \frac{1}{k_{r,A}K_A}\frac{1}{C_A} \tag{2}$$

provides an easy way to estimate the involved parameters, by making rate measurements at different concentrations. To reduce uncertainties, it is common to apply the method of initial rates to this equation, that is, to plot the reciprocal of the initial rate ($1/-r_{A0}$) versus the reciprocal of the initial concentration ($1/C_{A0}$) for various initial concentrations of the pollutant. Then, $k_{r,A}$ and K_A are estimated from the intercept and slope of the graph. The initial rates at specific initial concentrations are usually obtained by extrapolating concentration–time runs back to time zero. It was argued that the initial rate method suffered from a serious drawback due to the subjectivity in estimating the initial rates and that the method was in particular inadequate for multicomponent systems. Accordingly, a technique based on a well-known method of nonlinear estimation

[the Box–Draper technique (Box and Draper, 1965)] was adapted for photocatalysis and successfully demonstrated in the photocatalytic degradation of TCE (Mehrvar et al., 2000).

Real life may involve the participation of more than one species in the photocatalytic process, due to existence of several pollutants in the feed and/or due to formation of intermediate products. In the simplest case, this can be described by a competitive adsorption over one type of sites, such that the disappearance rate of specie i can be given by

$$(-r_i) \equiv -\frac{\mathrm{d}C_i}{\mathrm{d}t} = k_{r_i}\vartheta_i = \frac{k_{r_i}K_iC_i}{1+\sum_j K_jC_j} \tag{3}$$

A common example of the use of this type of equation is the considering of water molecules as competitive adsorbates (Junio and Raupp, 1993; Peral and Ollis, 1992).

The photocatalytic degradation of gaseous ethanol involves the formation of acetaldehyde as the main gaseous intermediate product (Vorontsov et al., 1997). It was found that in this case, fitting the kinetic data to a one-site model gave a very poor fit. Instead, a three-site photocatalytic model was proposed (Vorontsov and Dubovitskaya, 2004), following a previous work (Muggli and Falconer, 1998), which found that there were sites available only for acetaldehyde, sites available for both acetaldehyde and ethanol, and sites available only for ethanol. According to this model

$$(-r_{\mathrm{ET}}) = (-r_{\mathrm{ETEX}}) + \frac{k_{\mathrm{ET}}K_{\mathrm{ET}}C_{\mathrm{ET}}}{1+K_{\mathrm{ET}}C_{\mathrm{ET}}+K_{\mathrm{A}}C_{\mathrm{A}}} \tag{4}$$

$$(-r_{\mathrm{A}}) = \frac{k_{\mathrm{A}}^{\mathrm{A}}K_{\mathrm{A}}^{\mathrm{A}}C_{\mathrm{A}}}{1+K_{\mathrm{A}}^{\mathrm{A}}C_{\mathrm{A}}} + \frac{k_{\mathrm{A}}K_{\mathrm{A}}C_{\mathrm{A}}}{1+K_{\mathrm{ET}}C_{\mathrm{ET}}+K_{\mathrm{A}}C_{\mathrm{A}}} \tag{5}$$

where $(-r_{\mathrm{ET}})$ and $(-r_{\mathrm{A}})$ are the rate of disappearance of ethanol and acetaldehyde, respectively. K_{ET}, k_{ET} and K_{A}, k_{A} are the adsorption constants and the rate constants of ethanol and acetaldehyde, on sites that are available for both. $(-r_{\mathrm{ETEX}})$ is the ethanol photocatalytic oxidation on sites not available for acetaldehyde, and $K_{\mathrm{A}}^{\mathrm{A}}$, $k_{\mathrm{A}}^{\mathrm{A}}$ are the adsorption constant and the rate constants of acetaldehyde on sites that are available only for acetaldehyde. A clear asymmetry is noticed in Vorontsov's model between the expression for ethanol and the expression for acetaldehyde. This asymmetry was rationalized by a competition between ethanol and surface intermediate products, such as acetic acid (Muggli et al., 1998).

Water adsorbed on TiO_2 is the source for hydroxyl radicals needed to initiate photocatalytic reactions. On the other hand, water competes with the pollutants on adsorptive sites. It is for this reason that one finds out that the

performance of photoreactors varies significantly with the humidity, having a maximal efficiency at some intermediate level, which depends on the adsorpticity (capability of adsorption) of the contaminants as well as on the reaction pathway. For example, the photodegradation rate of *m*-xylene was found to increase with humidity up to 7% RH. Further increasing of the relative humidity caused a gradual decrease in the degradation rate (Peral and Ollis, 1992). In general, this optimal point is obtained already at a very low relative humidity, such that within the practical range of use, water acts to reduce the photodegradation rates of most contaminants. Increasing the initial concentration of the pollutants may shift the optimal point toward higher RH values (Obee and Brown, 1995).

A major obstacle for large-scale implementation of photocatalysis stems from the fact that photodegradation kinetics depends to large extent on the adsorption coefficient of the contaminants on the photocatalyst surface, such that it is extremely difficult to pohotodegrade molecules that hardly adsorb on the polar TiO_2. Unfortunately, many hazardous contaminants, in particular contaminants of low polarity, belong to this category. Moreover, in practice, the effluents that are needed to be treated contain several contaminants that compete on the adsorptive sites of the photocatalyst, thus limiting the validity of laboratory scale, single-component experiments, for practical use. These problems can be aggravated by lack of control on the formation of harmful by-products and toxic intermediates.

Attaching photocatalyst particles to inert domains may assist in improving the efficiency of the photocatalytic process. The basic concept, termed as "Adsorb & Shuttle," is based on using the inert domains for adsorbing target compounds that otherwise hardly adsorb on the photocatalyst. That way, a reservoir of the contaminants within a small distance from the photocatalytic sites is formed. Once adsorbed in the vicinity of the photocatalyst, the target molecules may surface-diffuse to the photocatalytic sites as shown schematically in Figure 5.

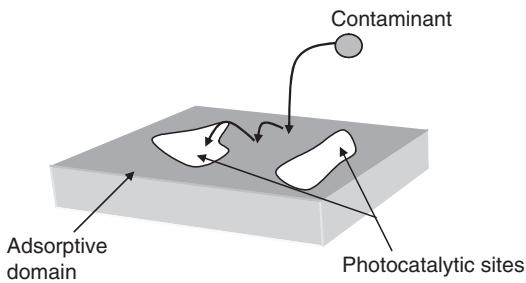

Figure 5 The concept of Adsorb and Shuttle.

Two typical gas-phase examples are the photocatalytic degradation of gaseous pyridine over a zeolite-supported titanium dioxide (Sampath et al., 1994) and the photodecomposition of propionaldehyde in air by a composite material made of titanium dioxide and activated carbon (AC) (Yoneyama and Torimoto, 2000). The photocatalytic activity of the composite photocatalysts was assessed by probing degradation kinetics and product distribution of the model contaminants. It was established that composite photocatalysts affect not only the degradation rates but also the distribution of intermediate products as well as the distribution of end-products. The extent by which these effects are manifested is governed by a large number of factors such as the surface area, the adsorpticity of the surface, the loading, the domain size, and even operational parameters such as humidity or temperature.

Too strong interaction between the adsorbate and the adsorbent might harm the diffusibility of the contaminant, thus canceling any synergistic effect. This was exactly what was found to happen at the photodegradation of dichloromethane on a composite photocatalyst consisting of titanium dioxide and AC (Torimoto et al., 1997). Here, the rate of CO_2 production was found to decrease monotonically with the increasing of the mass ratio of AC in the composite photocatalyst, even when the comparison was made on an equal amount of TiO_2 basis. In other words, in this case, not only that adding the inert adsorbent did not have any benevolent effect on the degradation rate, but, in fact, it competed against the photocatalyst, thus reducing the mineralization rate instead of enhancing it.

It is noteworthy that a large number of material-related parameters govern the activity of titanium dioxide in the gas phase. Among these parameters, one may outline chemical purity, phase (anatase or rutile), defect concentration, crystal size, porosity, surface area, and even aggregate size and particle–particle interaction (Ibrahim and de Lasa, 2002). In principle, these factors are basically the same as those in the aqueous phase and therefore will not be discussed at length within this chapter. We are not aware of any systematic work on a possible correlation between specific forms of titanium dioxide and specific types of use. However, it should be noted that, regardless of the experimental conditions, no shortage of oxygen can be expected for air treatment (unlike the situation with water containing high concentration of pollutants). At the same time, hydroxyl radicals are expected to be more abundant in the aqueous phase, hence the odds that a specific pollutant will be degraded by a direct mechanism of hole oxidation are larger in air treatment than in water treatment.

3.2. Mass transport

Mass transport, whether external (transfer from the bulk to the external surface of the photocatalyst) or internal (transfer within the pores of the

photocatalyst), can, in principle, limit the overall degradation rate of pollutants. It seems that most experiments where photocatalysis was applied for the decontamination of air did not involve mass transfer limitations conditions and were dominated by reaction kinetics rather then mass transport. An example is the degradation of methanol and TCE in both a tube reactor and in an annular reactor, where the reaction rate was found to be independent of the gas flow rate (within the experimental range) (Doucet et al., 2006). One of the few cases where mass transfer did limit the overall degradation rate was presented by Sclafani et. al. (1993), who oxidized phenol in a fixed bed annular photoreactor and observed that the reaction rate was strongly dependent on the flow rate of the feed.

To check for internal mass transfer limitation, it is possible to use the nondimensional Weisz modulus, φ', which is a modified version of the Thiele modulus (Levenspiel, 1998):

$$\varphi' \equiv \frac{r_V \tau L^2}{D C_S \varepsilon} \tag{6}$$

Here, r_v is the experimental mean rate of reaction per unit volume of catalyst, L is a characteristic length of the porous photocatalyst (i.e., the film thickness), τ is the pore tortuosity (taken as three), D is the diffusion coefficient of the pollutant in air, C_s is the mean concentration at the external surface, and ε is the catalyst "grain" porosity (0.5 for Degussa's P25). Such a treatment was performed by Doucet et al. (2006) while taking D of the pollutants to be approximately 10^{-5} m^2 s^{-1}. The estimated Weisz modulus ranged between 10^{-3} and 10^{-5}, depending on the type of pollutant, that is, some three to five orders of magnitude smaller than the value of unity, which is often taken as a criterion for internal mass transport limitation.

3.3. Light sources

Light sources are among the most important parts of photocatalytic devices, based on the fact that photons are often regarded as the most expensive component of photocatalytic reactors (Nicolella and Rovatti, 1998). Hence, it is obvious that criteria for effective use of photons should be very important in the design and operation of photocatalytic devices. Unfortunately (or not), the odds that lamp manufacturers will produce UV lamps especially designed for photocatalysis for a competitive price are very slim. As a consequence, the design and even the size of a feasible reactor is very much constrained by the commercial availability of the radiation source (Imoberdorf et al., 2007).

Indoor air treatment is usually done with artificial light, whereas outdoor treatment is considered to be a solar light-induced process [maybe except

for highway tunnels (Fujishima et al., 1999)]. Unlike water treatment, where light concentrators are sometimes in use (Monteagudo and Duran, 2006), air-treatment reactors rarely use concentrated light, following (sometimes unknowingly) the observation that above 1–2 mW cm^{-2} the quantum efficiency decreases with increasing UV flux. At any case, means for prevention of photon loss, such as mirrors, are quite common.

The most popular UV light sources are mercury plasma lamps, although sodium, zinc/cadmium, neon, and argon can be found in the market. The mercury lamps, emitting mostly in the UV-C range (200–280 nm), can be classified according to their pressure (Bolton et al., 1995). Low-pressure sources are characterized by short wavelength (80% of their output around 254 nm), long life time ($>$ 5,000 h), 30% energy conversion, and very low energy density ($\sim$ 1 W cm^{-2}). Medium pressure lamps have shorter life time ($\sim$ 2,000 h.), broad output range, moderate energy density ($\sim$ 125 W cm^{-1}) but low energy conversion ($\sim$ 15%). High-pressure mercury lamps have a life time of $\sim$ 3,000 h, with strong emission below 250 nm, high energy density ($\sim$ 250 W cm^{-1}), and high energy conversion ($\sim$ 30% into 200–300 nm light).

UV-A (315–400 nm) radiation is also used. In that case, the light is usually obtained by fluorescence caused by a mercury-lamp emission, using fluorescent media such as lead-doped barium silicate, europium-doped strontium borate, or europium-doped strontium fluoroborate. In addition, one may still find lamps that utilize the slightly broadened 365 nm spectral line of mercury from high pressure discharge. The UV-A lamps are often coated with a nickel-oxide-doped glass (Wood's glass), which blocks the visible light almost completely.

To large extent, the scientific literature is at least partially silent with respect to the effect of wavelength on photocatalysis. At most, there is some consideration to the fact that the absorption coefficient for 365 nm photons is significantly smaller than that for 254 nm photons, hence a thicker layer of photocatalyst is required with the former. Another effect of the shorter wavelength is the potential formation of active species that might play a role in the photooxidation reaction.

Accurate measurement of photon flux is essential in order to calculate quantum efficiency (whether based on absorbed photons' flux or the flux of photons impinging on the surface). The response of commercial sensors is wavelength dependence, hence, the readout, which is in energy flux units (W cm^{-2}), is usually calibrated according to either the 365 nm line of mercury or the 254 nm line, depending on the sensor. For more details on radiation sources see de Lasa et al. (2005). A different method for measuring photon flux is actinometry. This method was very popular in the past, however, very few researchers still use it due to its complexity and the time it consumes.

The efficiency of reactors is often given in terms of quantum yields (also called quantum efficiencies). One may find in the literature three types of

quantum efficiencies, as outlined hereby. The primary quantum yield (PQY) is defined as the number of molecules degraded from a primary process over the number of absorbed photons (Cassano et al., 1995). The overall quantum yield (OQY) is defined as the ratio between the total number of pollutant molecules degraded via both primary and secondary processes over the total number of absorbed photons. Both PQY and OQY are often measured at initial conditions. Determining the exact number of absorbed photons is not easy, due to the diffused and specular reflectivity of the photocatalyst surface. For this reason, a third term [apparent quantum yield (AQY), also called global quantum yield] is often used. It is defined as the number of converted reactant molecules over the number of photons entering the reactor (Fox and Dulay, 1993). For more details about the definition of quantum yields see de Lasa et al. (2005). In many cases authors use the term "quantum efficiency" or "quantum yield" without defining whether they refer to PQY, OQY, or AQY. This is very unfortunate as the quantum efficiency is one of the major parameters when comparing different reactors.

As will be discussed later in this chapter, the geometrical attributes of photocatalytic reactors are closely related to the geometry and irradiance of existing UV sources. It is for this reason, that a large portion of the scientific efforts in developing models for photocatalysis was concentrated and is still concentrated in trying to model the distribution of light intensity at the surface of the photocatalyst, taking into account absorption and multiple scattering and in calculating the penetration depth of the light. Most of these models were constructed to meet specific geometrical designs (annular, tubular, etc.) or specific modes of introducing the catalyst (packed bed, coated film, etc.) and are discussed in the following parts according to the specific types of reactors.

4. TYPES OF TARGET POLLUTANTS

The number of gas-phase pollutants whose photocatalytic degradation was studied is quite large. Some of these pollutants such as aromatic compounds, chlorinated olefins, hydrocarbons (Obee and Brown, 1995), aldehydes (Chin et al., 2006), ethers (Araña et al., 2008) and alcohols (Tsuru et al., 2006) can be found indoor at sub-ppm level. Others, like NOx, are more typical for outdoor environment. The main groups are probably volatile aromatic compounds belonging to the BTEX family and short chlorinated hydrocarbons, like TCE. Figure 6 presents the estimated annual number of scientific publications on the photocatalytic air treatment of NOx, BTEX, and TCE based on SciFinder Scholar^{TM} hits. These compounds were chosen based on the fact that they belonged to different chemical classes. NOx is representative for nonorganic compounds, BTEX

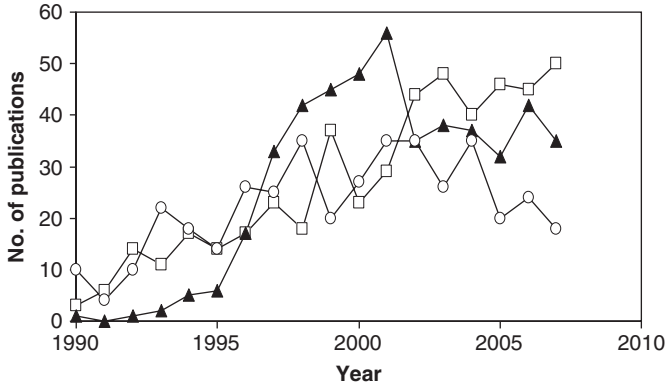

Figure 6 Estimated annual number of scientific publications, on the photocatalytic air treatment of NOx (filled triangles), BTEX (empty squares), and TCE (empty circles).

represents compounds that are degraded by hydroxyl mechanism, and TCE represents a specific case, where very high apparent quantum efficiency (AQE) is obtained due to radical chain reaction. In this context, it is noteworthy, that radical chain reaction leading to quantum efficiencies (OQY and even AQY), greater than 100%, are not limited to chlorinated compounds, as they were observed also for nonchlorinated molecules such as acetaldehyde (Ibrahim and de Lasa, 2003).

According to the figure, during the first years of research BTEX and TCE were more popular than NOx; however, over the years the importance of NOx in terms of publications was increased such that more and more scientific efforts were directed toward its degradation. As for TCE, it seems that it lost some of its early years popularity, most likely due to regulations that limited its use and consequently also its long-term potential threat. In the following part, the characteristics of these three gases as well as the main scientific findings regarding their photocatalytic degradation are discussed.

4.1. BTEX

Benzene, toluene, ethylbenzene, and xylenes (known as BTEX) are probably the most widely used aromatics, in abundant use in automotive fuel, as solvents or as feedstock for more complex compounds. The American Occupational and Safety Administration (OSHA) permissible exposure limit for benzene, for example, is as low as $3.26\,mg\,m^{-3}$ (1 ppm) due to its carcinogenic nature. This value should be compared with the $10–100\,\mu g\,m^{-3}$ of BTEX typically found in urban outdoor environment (Saarela et al., 2003). The photocatalytic degradation of BTEX might emit a variety of intermediate products and by-products. For example, the photocatalytic degradation

of xylene was found to release benzaldehyde, 2,5-furandione, methylbenzaldehydes, methyl benzoic acid, benzene dicaboxaldehyde, and 1,3-isobenzofurandione (Blanco et al., 1996). It is known that the concentration of pollutants might have a significant effect on the appearance and distribution of intermediate products as well as of end-products. This statement is in particular true for aromatic compounds, where low aromatic concentration has been shown to produce complete oxidation with little or no production of gas-phase intermediates (Ibsuki and Takeuchi, 1986; Obee and Brown, 1995), in contrast to degradation of 1.3 mol% in air, which led not only to the appearance of high concentrations of benzaldehyde but also to the production of benzene, benzyl alcohol, benzoic acid, and phenol (Martra et al., 1999).

As a consequence of the production of strongly adsorbed intermediates, the degradation of aromatics might not obey an apparent LH expression (Doucet et al., 2006). More important than the alteration of the kinetics expression is the gradual decrease in the degradation rate due to deactivation of the catalyst during continuous operation (Lewandowski and Ollis, 2003). The reason of deactivation is the formation of strongly bound intermediate products, which accumulate on the catalyst surface. The exact nature of these recalcitrant species is not always known. Even for toluene, whose degradation was studied intensively by numerous groups, there is still some debate on what are the chemical species responsible for deactivation, often accompanied by discoloration of the photocatalyst. Some researchers claimed that benzoic acid is the intermediate product to be blamed (Mendez-Roman and Cardona-Martinez, 1998), whereas others claimed that benzoic acid was not recalcitrant enough (Larson and Falconer, 1997). There is also a report on a mixture containing benzoic acid, benzyl alcohol, benzaldehyde, 4-hydroxybenzyl alcohol, 4-hydroxybenzaldehyde, and 3-hydroxybenzylaldehyde (d'Hennezel et al., 1998). In any case, whatever the actual recalcitrant species are, it is accepted that the aromatic ring structure was retained (Blount and Falconer, 2001).

Some regeneration was possible when the photocatalyst was exposed to UV in the presence of dry air (Luo and Ollis, 1996). However, this regeneration did not last for more than a few cycles, as the deactivation became irreversible, most likely due to accumulation of benzoic acid on the surface of the photocatalyst.

Overall, the BTEX compounds are among the most problematic pollutants, as they are both hazardous, quite abundant, and very difficult to handle.

4.2. Trichloroethylene

Trichlotoehtylene is a well-known pollutant. In aqueous systems this pollutant, like other chlorinated compounds such as chloroform, might be introduced into water following standard antibacterial treatment of drinking

water by chlorine. In the gas phase, its main sources are related to its superb ability to dissolve organic compounds, hence is used in a variety of applications, from dry cleaning to the microelectronic industry.

The photocatalytic degradation of TCE was studied intensively, both in the liquid phase and in the gas phase. Unlike in the aqueous phase, where the quantum efficiency is no more than a few percents (Alberici and Jardim, 1997; Pruden and Ollis, 1983), the quantum efficiency in the gas phase can be higher than 100% (Upadhya and Ollis, 1998). This difference was attributed to the existence of two mechanisms. That the mechanism in the liquid phase was different than that in the gas phase could be deduced also by the fact that the intermediate products dichloroacetaldehyde (DCA) and dichloroacetic acid (DCAA) were identified only during liquid-phase photocatalysis (Pruden and Ollis, 1983).

The photocatalytic degradation of TCE was studied in the gas phase for the first time by Dibble and Raupp (1990, 1992). A positive order was found with respect to the molar ratio of oxygen and TCE, whereas for water a negative order of reaction was observed. No intermediate products were observed. It was clear that traces of water were required in order to preserve photocatalytic activity for long time, however, high relative humidity reduced the reaction rate. The rate could be described by a modified LH equation:

$$R = k'\left\{\frac{K_1 y_{\mathrm{TCE}}}{1 + K_1 y_{\mathrm{TCE}} + K_3 y_{\mathrm{H_2O}}}\right\}\left\{\frac{K_2 y_{\mathrm{O_2}}/y_{\mathrm{H_2O}}}{1 + K_2 y_{\mathrm{O_2}}/y_{\mathrm{H_2O}} + K_4 y_{\mathrm{H_2O}}}\right\}^2 \qquad (7)$$

where $K_1 - K_4$ are constants, and y_i represents the molar ration of component i. Phillips and Raupp (1992) studied the mechanism of the photocatalytic oxidation of TCE and concluded that UV-induced water desorption was a prerequisite for TCE adsorption and degradation. In fact, pre-exposure of the photocatalyst to UV light in the absence of any pollutants for some time may increase the photocatalytic degradation rate of TCE by a factor of 3.5 (Kim et al., 1999a, b).

The photocatalytic degradation of TCE could be performed very efficiently, with reported quantum efficiency values that could reach 40–90% in a fixed bed reactor (Yamazaki-Nishida et al., 1993). It is noteworthy that the quantum efficiency based on mineralization was quite smaller (4–17%) than the quantum efficiency based on degradation.

A thorough work on the photocatalytic oxidation of TCE was performed by Nimlos et al. (1993), who identified, apart from CO_2 and HCl, also Cl_2, dichloroacetyl chloride (DCAC ($CHCl_2COCl$)), CO, and phosgene ($COCl_2$), known to be much more toxic than TCE. The high quantum efficiency observed in this case (50–80%) was attributed to a chain reaction initiated by the formation of chlorine atoms, similar to the scheme proposed for the

homogeneous case (Sanhueza et al., 1976). The chlorine atoms are formed following an attack of OH radicals on the TCE molecules:

$$CCl_2{=}CHCl + OH\bullet \rightarrow \bullet CCl_2CHClOH \quad (8)$$

$$\bullet CCl_2CHClOH + O_2 \rightarrow \bullet OOCCl_2CHClOH \quad (9)$$

$$2\bullet OOCCl_2CHClOH \rightarrow 2\bullet OCCl_2CHClOH + O_2 \quad (10)$$

$$\bullet OCCl_2CHClOH \rightarrow CHClOHCCl(O) + Cl\bullet \quad (11)$$

The chlorine atom attacks another TCE molecule to form an alkyl radical, which reacts with oxygen, thus forming a peroxo radical. Two peroxo radicals form the alkoxy radical, which reacts with a second peroxo radical yielding the alkoxy radical $CHCl_2CCl_2O\bullet$. This in turn may release chlorine to form DCAC or alternatively cleave a C—C bond to form phosgene (CCl_2O). The same group found, at a different study, that if the contact time is long enough, the phosgene may be hydrolyzed to yield CO_2 and HCl (Jacoby et al., 1994). It was further established that the product distribution is affected by the humidity. Increasing humidity increases the ratio between CO_2 and phosgene and reduces the mole fraction of DCAC in the product stream. However, this beneficial effect may come at the expense of reducing the overall rate of TCE degradation.

It should be pointed out that other groups (Fan and Yates, 1996) presented a contradictory explanation, based on using $^{18}O_2$ in the gas phase and monitoring the evolved CO_2, according to which the photocatalytic degradation of TCE was due to activated adsorbed oxygen and not due to hydroxyl radicals.

Nimlos et al. (1993) have found that the dependence of the gas-phase oxidation of TCE on the UV intensity, which was linear at high concentrations of TCE, changed its dependence into a square root law when the concentrations were low. This was explained (Upadhya and Ollis, 1998) by a change in the mechanism: at high concentrations the mechanism was a chain reaction mechanism induced by chlorine atoms, whereas at low concentrations the mechanism is the common holes/OH attack mechanism. This hypothesis correlated well with the fact that the quantum efficiency at high concentrations of TCE was 4–10 times higher than at low concentrations.

Treatment of an air stream containing high concentrations of TCE led to the deactivation of the photocatalyst. Several groups have reported that the surface of the photocatalyst became saturated, and as a consequence the amount of intermediate products that were released was increased (Driessen et al., 1998). The adsorbed specie was identified as dichloroacetate, which together with HCl is formed from DCAC reacting with hydroxyl

radical (Hwang et al., 1998; Larson and Falconer, 1993). The activity of the photocatalyst was restored by flowing humid air in the dark for short time (Dibble and Raupp, 1992).

4.3. NOx

Nitrogen oxides (NOx) such as nitric oxide (NO), nitrous oxide (N_2O), and nitrogen dioxide (NO_2) make one of the most common groups of air pollutants. They are released mainly from internal combustion engines and furnaces and are considered to be harmful atmospheric pollutants, as they can cause acid rain, photochemical smog, and greenhouse effects (Zhou et al., 2007).

It has been established that photocatalysis may oxidize NO into NO_2 and eventually to HNO_3 (Hashimoto et al., 2000). The HNO_3 may remain on the surface of the catalyst; however, it can be washed easily by water. It is no wonder, therefore, that photocatalysis is considered to be one of the most promising techniques to handle this outdoor pollutant. It was found that the release of NO_2, an intermediate formed during the oxidation of nitric oxide, is reduced upon immobilizing the titanium dioxide on AC (Ao and Lee, 2005). It was claimed that the mechanism of NO oxidation involves two steps. In the first step, the NO is attacked by OOH to form NO_2 and hydroxyl radical, whereas in the second step the OH radical oxidizes the NO_2 thus forming HNO_3. The role of the AC is therefore to adsorb the NO_2 and to shuttle it to the photocatalytic domains. In this context, it is noteworthy that the competitive adsorption of water, which is the main cause for the adverse effect of humidity at high RH, was reduced upon using composite photocatalysts, where the pollutants are first adsorbed on the inert domains and then diffuse to the photocatalytic sites (Ao and Lee, 2004). This finding was not altered in the presence of other copollutants such as benzene, toluene, *p*-xylene, ethylbenzene, or SO_2.

An interesting effect of low loading of titanium dioxide within a zeolite matrix can be the formation of end-products that differ significantly from those produced at high loading. This effect was demonstrated with the use of zeolite MCM-41 matrix, hosting 0.6% by weight of TiO_2 (Kitano et al., 2007). Here, photocatalytic removal of NO led to the formation of the more friendly reductive products (N_2 and O_2) instead of the usual oxidative products (NO_2, HNO_3). Results were explained in terms of the formation of isolated titanium dioxide, having a lower coordination number.

4.4. Mixtures

As mentioned above, an indoor environment contains a large number of pollutants, each at a ppb level. It is reasonable to assume that the coexistence of these compounds may alter not only the rate by which they are degraded

but also the type of by-products that are formed. The rate can be altered simply because of (the relatively easy to calculate) competitive adsorption, but also following interactions between intermediate active species. Despite the real need for the study of photocatalytic degradation of mixtures and the scientific challenge in understanding the related complex phenomena, the number of manuscripts on degradation of gas-phase mixtures is quite low. There are, however, several examples such as the study of mixtures of alcohols with their corresponding aldehydes (Araña et al., 2008) and a mixture of the four components of BTEX in equal amounts confirming that the activity order was benzene < toluene < ethylbenzene < *o*-xylene (Strini et al., 2005). It is for these reasons that the topic of mixtures was included explicitly in this chapter, thus conveying a message about the importance of studying mixtures in the context of photocatalytic air treatment.

The coexistence of various pollutants does not have to be deleterious, but, in certain cases, can be quite beneficial. The first evidence for this claim came probably from the work of Lichtin et al. (1994) who found that the edition of 0.03% by volume to an air-stream containing 0.1% iso-octane caused an enhancement in the photocatalytic oxidation of the latter. Likewise, a significant rate enhancement was recorded in the photocatalytic degradation of chloroform and dichloromethane in the presence of TCE. Similar effects were recorded also with other chlorinated olefins, such as perchloroethylene (PCE) and trichloropropene (TCP), which enhanced the photooxidation of toluene in a manner similar to that of TCE (Sauer et al., 1995).

The synergistic effect of TCE was attributed to a reaction with chlorine radicals formed during the decomposition of TCE. An extensive study of these observations, made by Luo and Ollis (1996), found that TCE concentrations higher than 225 mg m^{-3} promoted the oxidation rate of toluene (relative to its single component rate) as far as the toluene concentrations were lower than 160 mg m^{-3}. Higher concentrations of toluene acted to inhibit the decomposition rates of TCE. These findings were explained by an oxidation mechanism of TCE, which involved the TiO_2-aided formation of chlorine radicals. These radicals could induce a chain-reaction mechanism not only with TCE (thus preserving their concentration) but also caused a propagation reaction with molecules of toluene. When the toluene concentration was high, the consumption rate of chlorine radicals became so high that their concentration was reduced significantly and the TCE conversion fell accordingly.

The generality of the TCE-induced synergistic effect was studied later on in the co-oxidation of benzene, ethylbenzene, toluene, and *m*-xylene (d'Hennezel and Ollis, 1997). For all aromatic compounds, except for benzene, the rate of oxidation was enhanced in the presence of TCE; however, some decrease in the degradation rate of TCE was also noticed. As for benzene, no synergistic effect was observed; however, at the same time, the TCE degradation rate remained as it was in the absence of the copollutant. These results could be rationalized on the basis of a mechanism that operated

through the abstraction of hydrogen atom from the alkyl group attached to the aromatic ring, so no wonder there was no synergistic effect with benzene. Some synergistic effect was also found with acetaldehyde, 2-butanone, although at the expense of some reduction in the rate of TCE. The degradation rate of other copollutants (acetone, chloroform, methylene chloride, and 1,1,1-trichloroethane) was found to be reduced when TCE competed with them for the precious hydroxyls. Overall, the higher the surface coverage of the copollutant was, the more the TCE conversion was reduced. Such effect could be due to overconsumption of the chlorine radicals (the so-called kinetic effect) or due to blocking of TCE adsorption sites (the so-called thermodynamic effect).

5. PHOTOCATALYTIC REACTORS FOR AIR TREATMENT: MODES OF OPERATION

Photoreactors for air treatment require proper design, aimed at achieving high quantum yield for long operation time at minimal cost. For that, it is necessary to choose the right reactor's configuration, the right UV source and its location, and the right design of photocatalyst. Two modes of operation can be found: batch reactors and continuous flow, one pass, reactors.

5.1. Batch reactors (including recirculation systems)

Batch reactors are often used at laboratory-scale experiments, usually for studying reaction kinetics (Vorontsov and Dubovitskaya, 2004) or for demonstrating the efficiency of recently developed photocatalyst. Although their potential for industrial-scale treatment of air is very limited, they can still be quite useful for obtaining kinetic rates expressions.

Most of the batch reactors operate in a recirculation mode, where gas flows into the "working" volume, treated, and then recirculated. Recirculation reactors provide a uniform concentration of reactants and products inside the system, thus enabling the obtaining of reliable kinetic measurements. For example, closed reirculation system was used to study the effect of photocatalysis for inactivating bacteria in the gas phase as a function of air stream conditions (Goswami et al., 1997). A complete inactivation was found to be possible, provided that the humidity is within the range of 50% RH and that the flow rate was low enough.

A specific type of recirculating reactor is the commercial indoor-air treatment device. The device is characterized by a small operating volume (a few liters at most), which is several orders of magnitude smaller than the reservoir (a room, vehicle, or aircraft, for example). The reactor itself can be either free standing or part of a larger system, usually an air-conditioning system, and is supposed to be able to take care of continuous emission of

pollutants from construction materials as well as of short bursts of contaminants (Lewandowski and Ollis, 2003).

A word of caution needs to be added to this part on recirculating reactors, where the "working" volume is a very small part of the overall volume. As said before, recirculating reactors are, in essence, batch reactors (or semibatch in the case of inactivation of bacteria, if growth is allowed and nutrients are fed in). Therefore, one has to be very careful in using the terms of "contact time" or "retention time," while assigning them the same meaning as in continuous stirred tank reactor (CSTR) or plug flow reactor (PFR). Changing the flow rate, at a defined system, having a constant volume, has to do with changing the flow pattern and mass transport from the bulk to the film and should not be addressed as if the space time in a continuous reactor has been changed. It is unfortunate therefore that a small survey made by us revealed quite a few manuscripts suffering from this misconception.

Mixed flow reactors are quite rare in the context of gas-phase batch reactors. Nevertheless, they were used in several cases where it was essential to obtain uniform concentration of reactants at the photocatalyst's surface. Such cases include streams that contain very low level of pollutants (in the order of ppb), high conversion, and inadequacy of recirculating reactors due to parasitic adsorption of specific pollutants on the walls of the reservoir, the reactor, and the connecting tubes (Strini et al., 2005). Here, a cementitious photocatalyst was prepared by mixing P25 with a white cement powder, followed by the addition of water, hydration, humidity equilibration, and drying. The TiO_2 content in the cementitious material ranged between 0.5 and 6% on a dry cement basis. Linear dependence of the oxidation rate on pollutant's concentration was observed. A lower order was observed for the dependence of the catalytic activity on the TiO_2 loading, which was explained by formation of catalyst clusters.

5.2. Continuous, one-pass flow reactors

Continuous flow reactors are generally being in use whenever there is a continuous source of pollutants. These types of reactors are suitable in particular for handling process gases, thus reducing their release into the atmosphere. In such cases, it is expected to have at least some information on the composition and concentration of the pollutants in the inlet stream, which may assist significantly in designing the decontamination units.

Continuous flow reactors can also be found also at a laboratory scale, where the feed is constant and the output stream is constantly monitored by means such as GC-MS (Alberici and Jardim, 1997; Sun et al., 2007), GC-FID (Doucet et al., 2006), GC-TCD (Yamazaki–Nishida et al., 1996), or even FT-IR (Nimlos et al., 1993). In certain cases (for example: Doucet et al., 2006), continuous one-pass flow reactors are used for performing kinetic measurements later to be used for scaling up.

6. TYPES OF PHOTOCATALYTIC REACTORS FOR AIR TREATMENT

The photocatalytic reactors in use for air treatment can be categorized according to their gas flow geometry (tubular, annular, flat plate), according to the type of their light sources or according to the way by which the photocatalyst is introduced into the system. The preferred criterion is often a matter of personal taste and previous education. In order to summarize the various types a matrix was constructed, which represents the major types of photocatalytic reactors, care was taken in constructing this table, to assure that all the reactors mentioned in the Table 1 were in use for air treatment. For this reason, the fiber optic reactor (Peill and Hofffman, 1995), which was used for water treatment, was not introduced into the Table 1. The matrix is two dimensional (reactor geometry and catalyst form) since the third important dimension (light sources) is, to large extent, coupled to the other two dimensions. The fourth dimension, the photocatalyst itself and its manufacturing process, was not included here since a closed look at the data revealed a large collection of very specific production schemes and absence of data that could serve as a basis for true comparison or even generalization.

6.1. Tubular reactors

Tubular reactors are probably the most common photocatalytic reactors. Their popularity stems, most likely, from their simplicity. They are characterized by a gas flow along the axis of a tube, which contains the photocatalyst in many possible forms such as a thin coated film on its wall, fluidized particles, a coated monolith, or even as a free powder resting on an appropriate support. The light sources are located, in most cases, externally to the tube, in a parallel configuration relative to its axis. Reflecting surfaces encompass the lamps array, assuring that the only absorbance of photons would be that of the photocatalyst (Figure 7).

6.1.1. Powder layer tubular reactors

Powder layer reactors are based on an unattached layer of TiO_2 powder (usually Degussa's P25), deposited on a porous material such as glass. The flow of reactant vapors or contaminated air occurs in downward direction through the photocatalyst layer and the supporting frit. The catalyst load is usually adjusted to assure total absorption of photons, yet without limiting mass transport of contaminants. Illumination is preferably done from the front side of the photocatalyst-loaded frit to reduce the distance that the photoinduced charge carriers have to cross in order to reach the adsorbed pollutants. This type of reactor is so simple, and the replacement of used catalyst is so easy, that no wonder that this was one of the first types that were employed already in the seventies and the beginning of the eighties by

Table 1 Representative types of reactors, categorized by geometry and the way by which the photocatalyst is introduced into the reactor

	Tubular	Annular	Flat plate
Powder layer reactor	Lewandowski and Ollis, 2003; Peral & Ollis, 1992		
Fluidized bed	Dibble and Raupp, 1992	Lim et al., 2000; Lim and Kim, 2004; Matsuda and Hatano, 2005	
Coated wall, parallel flow	Araña et al., 2008; Doucet et al., 2006	Bouzaza et al., 2006; Doucet et al., 2006; Lim and Kim, 2004; Sidheswaran and Taviarides, 2008	Salvado-Estivill et al., 2007a,b
Packed bed	Araña et al., 2008; Tsoukleris, et al., 2007; Yamazaki-Nishida et al., 1996	Raupp et al., 1997; Stokke et al., 2006	
Plasma driven	Kim et al., 1999a, b; Sun et al., 2007; Thevenet et al., 2007		
Monolithic (honeycomb and foam)	Arabatzis et al., 2005; Blanco et al., 1996; Furman et al., 2007; Ibhadon et al., 2007; Nicolella, and Rovatti 1998; Nimlos et al., 1993; Obee and Brown, 1995		
Permeable layer	Tsuru et al., 2006	Ibrahim and de Lasa, 2002; Romero-Vargas Castrillon et al., 2006	

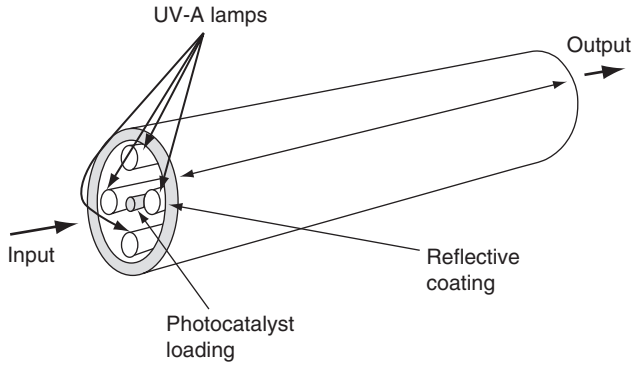

Figure 7 A schematic view of a tubular reactor.

Formenti et al. (1971) for partial oxidation of isobutane. This reactor was proved to be free of mass transfer problems and was regarded as an ideal reactor for laboratory kinetic studies.

As was pointed out justly by Lewandowski and Ollis (2003), powder layer reactors are not suitable for full-scale commercial application, as the high flow rate characteristic for commercial application might loosen the catalyst particles thus displacing the powder into the airstream or, in other cases depending on the configuration, might compress the bed, thus limiting the mass transport through the frit. Powder reactors are neither suitable for mobile or vibrating devices, as the vibrations might cause an uneven distribution of the powder, leading to channeling of contaminated air through the reactor with little contact with the catalyst powder, and in parallel, causing the formation of "dead volume" of photocatalyst at areas where accumulation of catalyst occurs.

6.1.2. Fluidized bed tubular reactors

Fluidized bed reactors (FBRs), characterized by an upward stream that is sufficient to lift and suspend the photocatalyst's particles, have several advantages. They enable high throughput of gas at a minor pressure drop, with very large contact surface between the pollutants and the photocatalyst. They are also very suitable for catalyst regeneration or replacement, an advantage that can be quite important for gas-phase pollutants that tend to deactivate the photocatalyst such as aromatic compounds or TCE (see Section 6.1, 6.2). No wonder that these reactors were among the first to be used (Dibble and Raupp, 1992), quite in parallel to the use of liquid–solid slurry reactors for water treatment. However, unlike the liquid-phase slurry reactors, they pose a real challenge in controlling the system – lifting the particles without carrying them out of the reactor. To succeed in this challenge, it is important that the particles have and maintain a proper size

distribution. Typical dimensions of fluidized bed catalyst particles in the chemical industry are in the range of 10–300 microns (Hill, 1977), if reasonable velocities are to be employed. This is much larger than the size of typical TiO_2 powders, hence supporting particulates should be required. Agglomeration is a known problem in FBRs, as the higher velocities needed for lifting the agglomerates might carry out the nonagglomerated particles. For the combination of air as an effluent and titanium dioxide as the particles, this problem seems to be of less importance. On the other hand, attrition of the solid, forming very fine powder that might be blown out of the reactor, should be of great concern for long-term operation. A separation unit, for example a cyclone, as in a Riser Reactor, seems to be essential.

One of the first fluidized bed photocatalytic reactors was presented by Dibble and Raupp (1992), who used silica-supported titania catalysts in order to degrade TCE with an AQE of 13%. Here, the UV sources in this bench-scale reactor were located externally to the reactor. Catalyst loss was prevented in this laboratory-scale reactor by introducing a second glass frit located at the reactor outlet.

6.1.3. Coated wall tubular reactors

Coated wall reactors are made of hollow tubes, coated with the photocatalyst on their inner walls, where the carrier gas flows. Coating of the catalyst may be achieved by impregnation in a TiO_2 suspension (approximately $2\,g\,L^{-1}$) (Araña et al., 2008) or by spraying of either a TiO_2 suspension or a TiO_2 precursor solution. The impregnation (or spraying) is usually followed by thermal treatment at elevated temperatures to improve adherence, and in the case of in situ preparation of the photocatalyst also to evaporate the solvent and to form the TiO_2 at the required anatase phase. The thickness of the photocatalyst film has to be sufficient to assure that almost all nonreflected photons are absorbed. This amount was found to be around $1\,mg\,cm^{-2}$ (Doucet et al., 2006). Higher loadings are not expected to assist, and might act to reduce efficiency, as layers that are too thick might, in the back-illumination case, reduce the number of photogenerated charge carriers which reach the front, active, surface.

The light source is located externally, either in front of the entrance to the tubes (front-type illumination on an array of straight tubes, relatively short) or in parallel to the straight tubes, illuminating from the back of the photocatalyst film. Another configuration is at the center of a spiral made from the tube around a (usually elongated, fluorescent type) UV light source. In that case, the photocatalyst is back-illuminated. Figure 8 schematically presents such a spiral reactor, used for the degradation of methyl tert-butyl ether (MTBE) (Araña et al., 2008). In the first configuration, there is no restriction with respect to the tube's material, as far as the photocatalyst adheres well to it; however, care has to be taken that the tubes are not too long, otherwise a "dead volume" is formed. The second configuration requires the tubes to

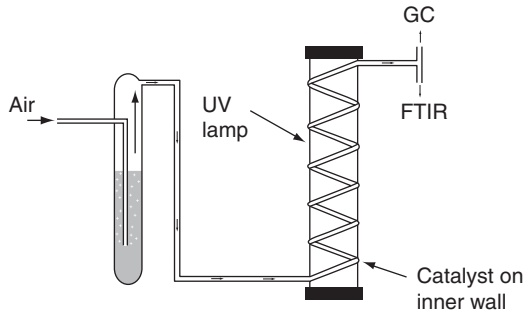

Figure 8 A coated wall tubular reactor in a spiral configuration (based on Araña et al., 2008; Vorontsov and Dubovitskaya, 2004).

be of a transparent material. If glass is used instead of silica and if the coating is made in situ by a sol-gel process, care has to be taken to prevent the migration of sodium ions from the glass into the nascent TiO_2 film (Paz et al., 1995; Paz and Heller, 1997). It is noteworthy that the spiral configuration, with its external light source, might suffer from inhomogeneous field of light impinging on the photocatalyst surface, the meaning of which might be less than optimal efficiency and difficulty in modeling the system.

A different configuration was presented by Doucet et al. (2006). Here, the catalyst (Degussa P25) was deposited on both sides of a pyrex glass plate, located inside a pyrex glass tube surrounded by six black fluorescence lamp. This front illumination reactor was used to study the degradation of TCE, methanol, and benzene.

6.1.4. Packed bed tubular reactors

Packed bed reactors are among the most used industrial reactors. However, they are of much less prospect for photocatalysis. PBRs are made of tanks or tubes, filled with photocatalyst pellets with reactants entering at one end and products leaving at the other. The gas flows in the void space around the pellets and reacts on the pellets. In the context of photocatalysis, the pellets can be made from inert materials coated with the photocatalyst or solely from titanium dioxide. This class may include, as many authors did, also columns packed with photocatalyst fine powder. A substantial complexity arises from the need to introduce the UV light into the packed bed. External light sources utilize only the outer part of the flow cross section, leaving a significant part of pellets in the dark. Assuming that some mixing occurs, the consequence is that large portion of the fluid might leave the reactor with much less "working" contact time that was considered by the designer. Three different PBRs, representing TiO_2 pellets, TiO_2 powder and spherules coated with TiO_2 are described herein.

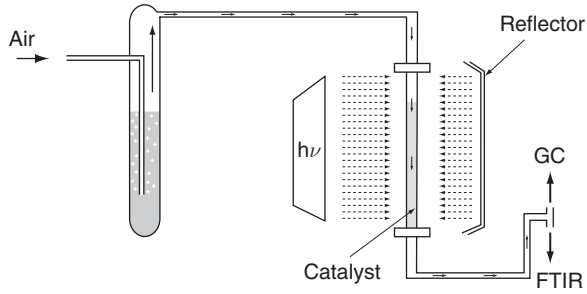

Figure 9 A scheme of the configuration of a tubular packed bed reactor (based on Araña et al., 2008).

Tubular reactor containing packed bed was used in a noncirculating mode to study the photocatalytic degradation of TCE and tetra-chloroethylene (Yamazaki-Nishida et al., 1996). The packed bed contained titanium dioxide pellets (1 mm in diameter), prepared by sol-gel and fired at 200–500°C. An inverse correlation between the firing temperature of the pellets and the formation of undesirable chlorinated compounds such as chloroform and carbon tetrachloride was found.

Packed bed reactors (Figure 9) with different lengths have been designed to study the photocatalytic degradation of MTBE, individual alcohols, and mixtures with their corresponding aldehydes. These studies have been performed with TiO_2 (Degussa P-25) and TiO_2 doped with Cu (Cu-TiO_2), the latter being more efficient than the former (Araña et al., 2008).

Another PBR introduced by the Tsoukleris et al. (2007) was based on glass spherules (0.5 cm in diameter) coated with a paste made of Degussa's P25, acetylacetone, and a binder (Triton X-100), which was then fired at 450°C to remove the organics and to improve the adherence. Photocatalytic degradation of BTEX with this reactor revealed remarkable stability, with practically no change in activity of the catalyst even after 30 consecutive tests.

6.1.5. Plasma-driven packed bed reactor

Plasma oxidation was suggested lately as a very promising way to treat VOCs in air (Oda et al., 1996, 2003). Efforts were made to study the effect of porous and various dielectric materials such as zirconates and titanates (Roland et al., 2002). It is no wonder, therefore, that the combination of titanium dioxide and plasma processes was tested as well.

A combination of packed bed titanium dioxide reactor and a plasma source was suggested as a means to obtain high efficiency and, more significantly, to reduce the appearance of undesired by-products. One of such designs (Kim et al., 1999b) utilized 5-mm pellets of TiO_2, packed in a quartz tube, into which a stainless wire held in its center served as a high-voltage electrode (Figure 10). The test gas contained, apart from N_2 as the

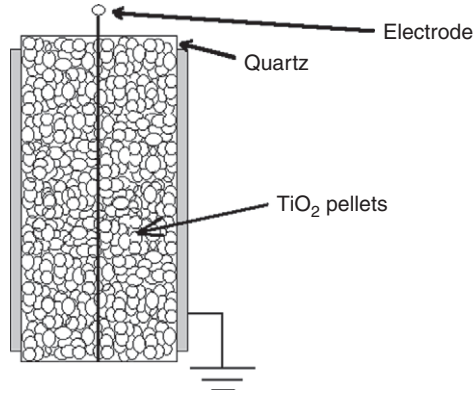

Figure 10 The plasma-driven reactor (based on Kim et al., 1999a).

carrier gas, also 400 ppm of NO, 10–15 ppm of NO_2, 10% O_2, and 1,000 ppm H_2O_2. The combination of discharge plasma with TiO_2 photocatalyst was found to be very effective for the removal of NOx by oxidizing it to HNO_3, in particular when H_2O_2 was added to the mixture. In addition, the emission of by-products, such as nitrous oxide (N_2O) or ozone, was significantly suppressed. It is noteworthy that the reactor did not contain a separate UV light source, so that photocatalytic contribution to the degradation was due to illumination by the plasma.

Plasma-driven photocatalysis was performed also for degrading gas-phase toluene (Sun et al., 2007), showing a significant increase in the removal of toluene, while decreasing the number of secondary by-products. It is noteworthy that the decrease in the emission of by-products could be also due to the loading of the photocatalyst on AC fibers, which could operate through the "Adsorb and Shuttle" mechanism (Paz, in press).

The synergistic characteristics of plasma-driven photocatalysis were studied also in the degradation of acetylene (Thevenet et al., 2007). Four modes of experiments were performed: photocatalytic, plasma degradation, plasma degradation + TiO_2 but without light, and a combined plasma and photocatalytic operation. It was found that plasma alone could not mineralize acetylene, as more than 50% of the carbon in the acetylene feed could not be accounted for, and, most likely, ended as strongly bound adsorbate by-products. Although the photocatalytic degradation per se was slower than that with plasma alone, the combination of the two was claimed to be very beneficial as it improved the mass balance of mineralized carbon (i.e., it reduced the formation rate of strongly bound by-products) and reduced the ratio between the production rate of carbon monoxide and that of carbon dioxide.

6.1.6. Monolith tubular reactor

Monolithic catalysts are solid structures pierced by parallel channels that facilitate the polluted air to flow through (Figure 11). The channels are usually wide enough to reduce the pressure drop by several orders of magnitude in comparison with powdered reactors. Moreover, if designed properly, in a manner that the light is guided into all the internal surfaces of the channels, monolithic reactors may provide a reasonable way to get quite a large area of exposure per source. The monolith itself may consist of a metal or oxide support, containing the photocatalyst either in the form of a coating layer or as a part of the matrix. Monolithic catalysts have been shown to be very suitable for gas contaminants treatment and are widely used in automotive emission control systems (Nicolella and Rovatti, 1998). Their large external surface and low pressure drop, together with a geometry that permits an increase in the lighted area, make them a very good candidate for commercial use. Monolith reactors are not affected by the problems that powder reactors have, with respect to separation between the photocatalyst fine-powdered particles and the gas stream. On the other hand, they are expected to be more expensive than the simple powdered reactors.

One of the first examples for the use of monolith reactors was presented by Blanco et al. (1996), who used a monolith made of titania dispersed in fibrous silicate to decontaminate air streams containing toluene or xylene, with a conversion up to 96% for toluene and 99% for xylene.

An alumina reticulate (4 channels cm^{-1}) was coated with Degussa P25 by simple wash-coat and used as a single-pass reactor (Obee and Brown, 1995) in order to study the effect of humidity on the degradation of formaldehyde, toluene, and 1,3-butadiene. The thickness of the reactor was 2 cm; however, the active depth was no more than 1 cm. For all three pollutants, the oxidation rate dependence on UV intensity within the range of 10–40 mw cm^{-2} followed a power law, with an exponent of 0.55. This was in agreement with previous works (Ollis et al., 1991; Peral and Ollis, 1992), which showed a linear dependence below 1–2 mW cm^{-2} and an exponent of 0.5 at higher intensities. Similar monolith, coated with P25, was used by Nimlos et al. (1993) to study TCE degradation. Parallel measurements were made by

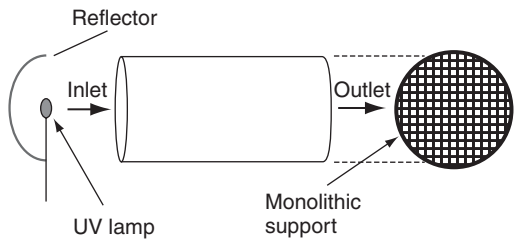

Figure 11 A schematic side view and front view of a monolithic photocatalytic reactor.

a film-on glass tube reactor. Both revealed the existence of by-products explained by radical chain mechanism induced by the formation of chlorine atoms.

The tubular monolithic reactor was a subject to quite a few models. One of the first models of honeycomb monolithic reactor was presented by Sauer and Ollis (1994). It assumes a CSTR reactor (the monolith) connected in series to a well-mixed recirculating loop, LH isothermal kinetics, and no mass transfer effects. It further assumed that the conversion per pass in the system was very low, that is, assumed a uniform concentration throughout the system. It should be mentioned that the model did not take into account the effect of radiation gradient along the pores and lumped all the radiation-related parameters. It did, however, make an estimation on the maximum active catalyst volume, taking into account the geometry of the pores, the geometry of the lamp, and its distance from the monolith. The model was validated for the degradation of acetone on a porous monolith (10 μm pore size) having 4-mm square channels, 15 cm in length, coated with P25 particles and operated under constant humidity conditions. The model showed very good predictive power at all conversions once the kinetic parameters were calculated based on initial rate measurements.

The influence of the geometry of the monolith on the reactor's efficiency was studied by Furman et al. (2007). A model, taking into account light absorption, hydrodynamic and transfer processes, and the reaction kinetics was developed. Three different geometries of the monolith reactor were tested: mixer, crossed channeled, and star. The monoliths were prepared by prefabricating an epoxy resin support using laser stereo lithography, followed by impregnation in P25 suspension. All three reactors had similar coated surface, of approximately $4 \times 10^{-3}\,m^2$. The model was analyzed assuming a very efficient external mass transfer, that is, that the surface concentration of the contaminant (methanol) was identical to the bulk concentration. LH kinetics were assumed, such that an apparent kinetic constant k could be calculated, taking K, the adsorption equilibrium constant as $129.7\,m^3\,mol^{-1}$ at 50°C, following published values. Under these assumptions, the apparent kinetic constant was 2.6×10^{-5}, 2.1×10^{-5}, and 1.7×10^{-5} (mol s^{-1}-m^{-2}) for the mixer, crossed channels, and star configurations, respectively. From this it was deduced that the mixer structure absorbs more photons per unit area of support than the two others. It is noteworthy that a good fit between the model and the experimental results was found only for flow rates higher than $0.2\,L\,min^{-1}$, indicating a mass transfer problem below this value.

A mathematical model of the operation of monolith reactors, focusing on the effect of light absorption on the heat and mass balance within the reactor and on the overall reaction kinetics, was presented by Nicolella and Rovatti (1998). The model assumed steady-state conditions, uniform pressure along the monolith channels, negligible axial diffusion, negligible conduction in the gas phase, and no homogeneous reaction. A circular dish lamp emitting

monochromatic light was assumed. It was further assumed that the emitted rays were focused in front of the monolith entrance, that the monolith channels were placed axially relative to the lamp, and that reflection and scattering were negligible. Out of the many assumptions that were made, the last assumption is probably the most problematic as both the refractive index of titanium dioxide and the angle that the UV light impinge on the monolith surface suggest that reflection and scattering might play a dominant role. It is noteworthy that although the energy balance equations were taken into account in the model, the authors did acknowledge the fact that the energy effects are practically negligible due to the low concentration of contaminants in the air stream.

A different type of monolith reactor, the so-called foam monolith reactor, was designed and fabricated by Arabatzis and Falara (2003) and Arabatzis et al. (2005) for the treatment of VOCs. This type of photoreactor had the advantage that the photocatalyst could be formed in situ inside the reactor, thus could be obtained very easily in any desired geometry. The monolith was located within a centered glass tube located in parallel to the axis of four UV lamps, arranged in a symmetrical manner, forming a cross. The foam (Arabatzis and Falara, 2003) was prepared by adding H_2O_2 to a paste made of P25 and a surfactant in acetone. The H_2O_2 decomposed, releasing molecular oxygen bubbles that acted to gradually increase the overall volume within an hour. The foam possessed a highly porous structure, with an extended network of interconnected flakes forming irregular polygonal cavities of 200–500 nm in size. This structure was attributed both to H-bond interaction between the hexadecylamine (HDA) surfactant molecules and the nanocrystalline titanium dioxide and to hydrophobic interactions between adjacent HDA molecules responsible for the formation of a lamellar structure.

The modeling of this type of reactor was presented by Ibhadon et al. (2007) and validated by measuring the degradation of BTEX. It was found that this type of reactor could be quite efficient at low concentration of pollutants; however, its rate constant as well as the pollutants' conversion dropped considerably at high (millimolar) concentration of pollutants. A major obstacle for practical use was the fragility of the foam, which suggested that the reactor might suffer from severe stability problems under prolonged use, as there is no guarantee that the network architecture of the pores would not change over time.

6.1.7. Permeable layer tubular reactors

Permeable layer reactors consist of thin, porous metal or ceramic substrates onto which titanium dioxide is coated in a manner that allows for flowing through the porous substrates. The flow can be either perpendicular to the surface of the porous media or alternatively may combine perpendicular and parallel vectors. An example of such a reactor was presented by Tsuru et al. (2006). Here, a titania membrane (pore sizes 2.5–22 nm) was prepared

by a sol-gel process, on the outer surface of an α-alumina microfiltration filter, using commercial anatase sol solution as an intermediate layer. The microfiltration filter was connected to a glass tube using glass frits, such that the air permeated through the membrane into the tube, from which it continued to a GC system equipped with thermal conductive detector (TCD). The membrane cell was positioned within a quartz tubular reactor, irradiated by eight black-light lamps. Photodeposition was used to dope the surface of the membrane with platinum using chloroplatinic acid as a precursor. An increase in the decomposition of methanol upon decreasing the pore diameter was observed and was attributed to better contact between the TiO_2 pore walls and the permeating reactants.

6.2. Annular reactors

Annular flow reactors are characterized by a cylindrical lamp surrounded by two concentric tubes such that the polluted air flows in the annulus between the inner and the outer tubes. That way, all emitted photons can be utilized without the use of expensive reflectors. In certain cases (Doucet et al., 2006), an optical (occasionally liquid) filter is introduced between the lamp and the flowing zone to control the wavelength and the power of the impinging light, as well as the temperature within the reactor.

6.2.1. Fluidized bed annular reactors

Fluidized bed reactor in an annular configuration was used for the study of NO (Lim et al., 2000) and TCE degradation (Lim and Kim, 2004). Here, P25 particles were attached to silica gel particles in order to improve their fluidization behavior. Light was introduced both from the center of the annulus and by affixing germicidal lamps outside of the reactor. The optimum phase holdup ratio of gas and solid phases for the TCE degradation was found to be 2.1, higher than values obtained for other photocatalytic FBR that used γ-alumina particles instead of silica gel, suggesting that silica gel is appropriate substrate for photocatalytic fluidization reactors.

A riser-type of FBR was presented by Matsuda and Hatano (2005) for the photocatalytic removal of NOx. Here, the FBR was coupled integrally to a cyclone-separating system that returned the carried-away titanium dioxide-loaded silica-gel particles.

6.2.2. Coated wall annular reactors

Coated wall annular reactors (Figure 12) are characterized by a thin film of photocatalyst located either on the outer side of inner tube or on the inner side of the outer tube. There are many reasons for preferring the inner side of the outer tube for the coating. The first reason has to do with the flux; it is known that at high flux of light (>1–$2\,mW\,cm^{-2}$) the quantum efficiency is proportional to 1 divided by the square root of the intensity. Hence, it is

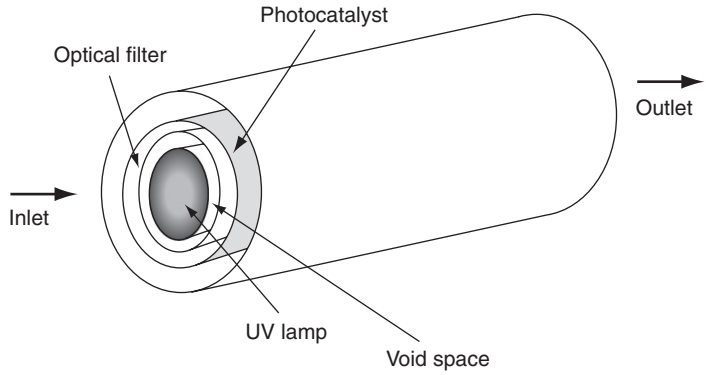

Figure 12 A typical annular flow reactor (after Doucet et al., 2006).

preferable to utilize the same number of photons per unit time on a larger area, as provided by the outer tube. The second reason has to do with the direction of illumination: for the inner tube the illumination is from the back side of the coating, whereas if the coating is the inner side of the outer tube, the illumination is at the front side of the photocatalyst. Still, many groups prefer to put the coating on the inner wall of the annulus.

It was shown that coated wall annular flow reactors can be modeled successfully as plug-flow reactors (Bouzaza et al., 2006). Here, the relative contributions of mass transfer and chemical reaction during the photocatalytic degradation were studied for two types of VOCs: TCE and toluene. A very simple steady-state model was used, following an approach developed previously (Ku et al., 2001; Lin, 2002). According to this model, which assumes LH kinetics, and under the assumption that the mass transfer in this PFR is not the limiting step, it is possible to describe the concentration of the pollutant along the reactor axis in the following very simple equation:

$$u\frac{dC}{dZ}+\frac{kKC}{1+KC}=0 \tag{12}$$

where $C(z)$ is the concentration in the bulk at an axial position Z, u is the flow velocity, k is the reaction rate constant (mol L^{-1} min^{-1}), and K is the Langmuir adsorption constant (L mol^{-1}). Integrating this equation provides (after some arrangements) a way to validate whether the system suffers from external mass transfer limitation or not, since in the absence of mass transfer limitation it is expected to have the following relation between the initial and the final concentration:

$$\frac{\ln\left(C_{in}/C_{out}\right)}{C_{in}-C_{out}}=\frac{kKL}{u(C_{in}-C_{out})}-K \tag{13}$$

where C_{in} and C_{out} are the concentrations of pollutant at the reactor's inlet and outlet, respectively, and L is the reactor length. Accordingly, if all assumptions are correct, a plot of $[\ln(C_{in}/C_{out})]/(C_{in}-C_{out})$ versus $1/[u(C_{in}-C_{out})]$ should be linear, and it should be able to calculate kK from the slope kKL. This provides a way to estimate the effect of mass transfer resistance by comparing kK with k^*, the apparent first-order rate constant. k^* is calculated separately by measuring the concentration at the outlet, since the reactor obeys the simple first-order reaction PFR equation:

$$\frac{C_{out}}{C_{in}} = \exp\left[-\frac{k^* L}{u}\right] \tag{14}$$

Estimating the effect of mass transfer resistance was done based on the connection between k^* and k:

$$\frac{1}{k^*} = \frac{1}{kK} + \frac{1}{k_m a_V} \tag{15}$$

where k_m is the mass transfer coefficient from the gas to catalyst surface ($m\,min^{-1}$) and a_V is the total effective catalyst area per unit volume of the reactor ($m^2\,m^{-3}$). Under the conditions of their experiments, the apparent rate constant (k^*) with toluene was very close in its value to the product kK, over a wide range of velocities (0.1–0.5 m s^{-1}), demonstrating that the resistance due to mass transfer was negligible.

It was already mentioned here that in back-illuminated film reactors (a class that includes annular film reactors), the performance as a function of film thickness is expected to go through a maximum. If the photocatalytic film is too thin, some of the photons might escape due to insufficient absorption and might not be utilized. If, however, the film is too thick, all photons will be absorbed, but lesser number of charge carriers will reach the surface due to the long distance between the location of charge carrier formation and the surface, which promotes charge recombination. For some reason, this point was somehow overlooked, and very few manuscripts give any attention to optimize the thickness of the photocatalyst film, such that one finds sometimes coatings having a thickness of 20 μm or so, at least 4–5 times thicker than the (wavelength dependent) optimal thickness.

6.2.3. Packed bed annular reactors

A two-flux radiation field model for an annular packed bed photocatalytic oxidation reactor was presented by Raupp et al. (1997). Similar to other annular flow reactors, the UV source was located at the center of the cylindrical reactor. Yet, the photocatalyst was not introduced in the form of a thin film but rather as spherules filling the annular space between the lamp and the housing. The principal assumptions made in this model included a steady state, isothermal operation, cylindrical symmetry,

uniform packing shape and distribution, plug flow, negligible radial and angular diffusion, negligible light absorption by the gas and dilute reactants (i.e., negligible heat of reaction and constant density). These assumptions led, in essence, to a pseudohomogeneous model. The radiation balance was solved first, under the assumption that there was no absorption by the gas and that the total UV irradiance at a given point was the sum of the forward and backward irradiances (i.e., back-scattering in the radial direction). The model was constructed for reactor walls made of nonabsorbing, nonreflecting material. This might be not so realistic since making the outer walls from a reflecting material (thus reducing photon loss) is commonly, and justly, done. The intensity profile of the UV light, calculated by a fourth-order Runge-Kutta method, was then used to solve the mass balance equations by a central finite difference method. Very good agreement between the model's predictions and the conversion of acetone was obtained, using 1 mm OD silica beads, onto which Degussa P25 was attached. It is noteworthy that the model suggested that radial gradient in the local volumetric rate of energy absorption (defined as mole photons per unit time per unit volume) in this configuration may lead to significant gradients in concentration and reaction rate, which ultimately might limit the reactor performance.

6.2.4. Permeable layer annular reactors

Similar to permeable layer tubular reactors, the permeable layer annular reactors are characterized by thin, porous substrates onto which titanium dioxide is coated in a manner that allows for flowing through the porous substrates. The flow can be either perpendicular to the surface of the porous media or alternatively may combine perpendicular and parallel vectors. The venturi reactor (also called the photo-CREC-air reactor) developed by de Lasa's group (de Lasa and Ibrahim, 2004; Ibrahim and de Lasa, 2002) followed this definition. This reactor was made of a venturi-like tube, containing a square basket covered with woven fiberglass screen, impregnated with TiO_2 on its side walls. The air flew through the venturi throat and around the basket base, and then contacted the impregnated mesh, where oxidation occurred, and continued its flow through the mesh. In a more advanced model (Romero-Vargas Castrillon et. al., 2006), several changes were introduced in the design: perforated plates replaced the wire-mesh basket, the front base of the basket received an aerodynamic shape, and cross section of the basket was altered from a rectangular shape into a cylindrical one. The flow took place between the TiO_2-impregnated screen and an outer house, thus forming an annular (or close to annular in the original scheme) flow cross section. A major difference between the annular flow reactors described above and the venturi reactor was the location of the UV lamps. In the annular reactors described above, the lamps were located at the center of the cylinder, along its axis, whereas at the venturi reactor the UV sources were mounted outside of the venturi divergent section, housed inside parabolic reflectors.

A commercial computational fluid dynamics (CFD) package (CFX-10) was used to solve the Reynolds-averaged mass, momentum, and contaminant transport equations under isothermal conditions (Romero-Vargas Castrillon et al., 2007). The process took into account the pressure drop, assumed a turbulent flow in the vicinity of the photocatalyst support, and a LH-type kinetics. The model contaminant was acetone, as this pollutant degrades photocatalytically without any observable gas-phase species except for carbon dioxide and water (Ibrahim and de Lasa, 2003). Significant differences were found between the two designs with respect to single-pass conversion values, which were attributed to both higher UV flux and available surface area in the advanced design.

6.3. Flat plate reactors

Flat plate reactors are characterized by a thin layer of photocatalyst-coated on a flat (or zigzagged) support, made of glass or metal, such that the flow of contaminated air is in parallel to the photocatalyst panel (Figure 13). The UV light sources can be either located within the embodiment of the reactor, or otherwise can be located externally to the reactor, introducing their light through a glass window. Care has to be taken to design the inlet and outlet in a manner that achieves uniform and fully developed flow over the photocatalytic plate (Salvado-Estivill et al., 2007a, b).

Flat plate reactors, being very simple for construction and analysis, are often used as a tool to obtain kinetic data, later to be used in the modeling of more complex system, for example, that of an annular reactor (Mohseni and Taghipour, 2004).

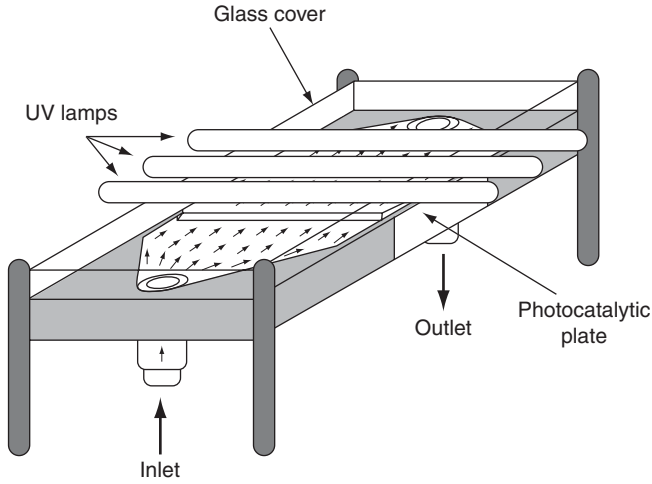

Figure 13 Schematics of a flat plate reactor (after Salvado-Estivill et al., 2007a, b).

6.4. Generalized models and comparisons between reactors

In the last years, there is a growing tendency to develop tools that will facilitate to simulate results for one type of a reactor by performing measurements on a different type of a reactor having a smaller size. Along this line, a first-principles approach that enables scaling-up was developed by Cassano's group (Imoberdorf et al., 2007) for reactors consisting of catalytic walls coated with a thin layer of titanium dioxide. The approach, which did not use any adjustable parameters, was demonstrated in the photocatalytic degradation of PCE. By utilizing kinetic information obtained in a laboratory scale, flat plate reactor operating at a steady state in a continuous, well-mixed recirculation reactor, it was possible to make very good (validated) predictions for a pilot-scale continuous, multiannular reactor having a catalytic surface 60 times larger than that of the flat plate reactor. The methodology was based on few principles: using fundamental chemistry research and detailed degradation mechanism, employing the same catalyst preparation protocol and morphology in both reactors, using a laboratory device as simple as possible to be operated under isothermal conditions, and most important, carrying the laboratory-scale experiments under the kinetic control regime (i.e., under conditions free of mass transfer limitations).

To large extent, the above-described method (as well as other scale-up methods) points into the importance of obtaining the complete kinetic network. Such an understanding involves measuring the time-dependent concentration of all species involved, that is, not only the reactant and the most common end-product (CO_2) but also the concentration of all intermediate products, as well as that of end-products other then carbon dioxide. Such a measurement can be quite problematic, taking into account that it is very rare to find a single experimental technique that would be suitable. In that case, choosing relatively simple model pollutants such as acetone or acetaldehyde (Ibrahim and de Lasa, 2004) might assist.

Computational fluid dynamics approach was utilized in the study of photocatalytic destruction of gas-phase vinyl chloride in an annular flow reactor (Mohseni and Taghipour, 2004). The kinetic data for the model was obtained from a differential glass plate reactor. The modeling results indicated significant gradient of vinyl chloride in the radial direction and nonuniform flow distributions, which resulted in reduced efficiency over the entire range of inlet concentrations.

Three-dimensional CFD-coupled with radiation field modeling and photocatalytic reaction dynamics was employed by Salvado-Estivill et al. (2007b) to model the decomposition of TCE in a flat-plate, single-pass photocatalytic reactor containing immobilized P25. The outcome was pollutant-specific kinetic rate parameters, which were independent of the reactor geometry, radiation field, and fluid dynamics. This was followed by

a two-dimensional model, which assumed fully developed laminar flow, uniform irradiation, large width to thickness ratio, negligible axial diffusion. The model coupled the photocatalytic reaction kinetics (prededuced from the 3D model) with unsteady state continuity equation and with a radiation field to give the transient and the steady-state behavior of the reactor (Salvado-Estivill, 2007a). Application of the model to the photocatalytic oxidation of TCE in humidified air streams closely approximated the experimental results, demonstrating the possibility to use a simple, less time-consuming 2D approach for computational modeling of such reactors.

This tendency for generalization goes to large extent hand in hand with the works of researchers, who are seeking the optimal configuration and design for air-treatment reactors. An example for this statement is a comparison between two PBRs and a coated wall reactor, both having a diameter of 4 mm (Araña et al., 2008). The two PBRs had a working length of 15 and 75 cm, whereas the length of the coated wall reactor was 140 cm. Each of the reactors utilized the same amount of photocatalyst (0.15 g), with approximately the same contact time. APQs defined as the ratio between the moles of MTBE that were degraded per s cm^2 and the moles of incident photons per s cm^2 were calculated. The APQ values were 0.009 with the coated wall reactor, 0.021 with the long PBR, and 0.03 with the short PBR. The differences were attributed to variations in the light penetration, since all other parameters had equal values. The importance of comparing between reactors is very well demonstrated in the case of TCE. Here, it was shown that the type of reactor may have a crucial effect on the product distribution as it affects the actual contact time. A coated wall annular reactor, used by Jacoby et al. (1994) yielded significant amounts of phosgene but no DCAC. In contrast, a PBR did not yield any phosgene (Yamazaki-Nishida et al., 1993). It was claimed that the different results were due to "dark" reaction taking place in the PBR, where the phosgene is hydrolyzed to HCl and CO_2. The fact that in both cases same relative amount of CO was obtained brought the researchers to claim that the released CO originated directly from the photocatalytic degradation of the TCE and not from the consecutive hydrolysis of the phosgene.

6.5. Combined adsorptive-photocatalytic reactors

One way to improve the performance of photocatalytic air-treatment reactors is to decouple between cleaning the air and degrading the pollutants. Figure 14 shows schematically such a system (Chin et al., 2006; Shiraishi et al., 2003). The system includes two independent continuous flow systems interconnected by a rotating, cylindrical ceramic honeycomb. The rotation cycles the honeycomb rotor through a low temperature zone, where adsorption takes place, and a high temperature zone where desorption takes place, thus regenerating the monolith. The contaminated air flows

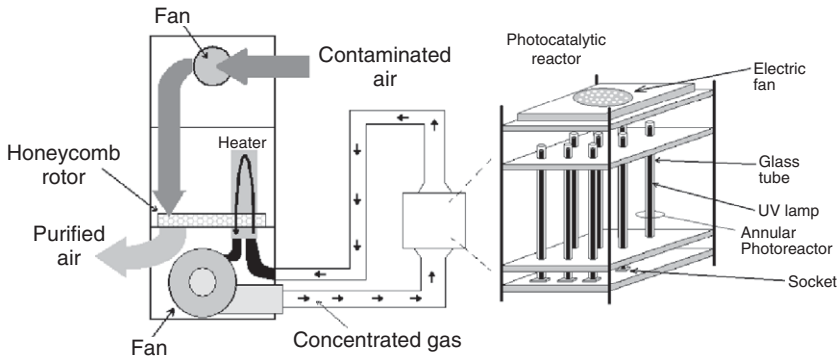

Figure 14 Schematics of a combined adsorptive-photocatalytic system (after Shiraishi et al., 2003).

through the monolith and leaves the device as a purified air. The pollutant (formaldehyde) that has been desorbed from the monolith is pumped in a recirculation manner to the so-called small box reactor, which comprises of nine coated- wall annular reactors.

The reactor was modeled by Chin et al. (2006) to determine adsorption, desorption, and pseudo-first-order rate constant. A photocatalytic rate constant, calculated based on the experimental data of Shiraishi and the model, was found to be in good agreement with previously published value.

7. CURRENT PROBLEMS AND FUTURE TRENDS

Taken the large number of groups and the diversity of topics, it is quite difficult to foresee the progress that will be made in this field in the next years to come. Yet, it is believed that it is possible, based on analyzing the current status, to pinpoint the current major bottlenecks in the photocatalytic treatment of air, while hoping that if these are indeed the major obstacles for large scale implementation and if these obstacles are recognized and defined, then a systematic research on these issues will eventually solve them. To some extent, this is an optimistic way of looking at scientific endeavors. We do hope that this optimism will justify itself.

7.1. Visible light

Constant efforts are being taken in the last years to shift the activity of titanium dioxide toward the visible by introducing dopants such as carbon, nitrogen, or iron. Although some literature exists on air treatment (Sidheswaran and Taviarides, 2008; Yin et al., 2008; Zhou et al., 2007), the

overwhelming majority of the experiments was done in the context of water treatment. This is simply due to the fact that water seems to be the natural candidate for the use of solar energy and therefore for such an improvement. Nevertheless, red shifting of the activity could greatly assist in the area of outdoor air cleaning. In the context of indoor air treatment, red shifting is unlikely to make revolutionary changes, although it may push forward indoor air treatment simply due to the promotion of the general field of photocatalysis. Direct contribution to indoor air treatment is, in our eyes, less likely to occur, although it should not be ruled out.

7.2. Mixtures

Taking into account the large number of manuscripts dedicated to photocatalytic air treatment, it is amazing how small is the number of scientific papers on the properties of mixtures of gases. This is despite the fact that indoor air contains always a mixture of pollutants, which might interact between themselves during photocatalysis. The partial data that is already in hand point toward the existence of synergistic mechanisms that could, in principle, be utilized to enhance degradation rates, if not in the context of indoor air (since the concentration in indoor air might be too low to get a significant change), then at least in the context of treating process gases.

7.3. Standardization

Intensive efforts have been made to develop new, modified photocatalysts. Likewise, a lot of skills and imagination were put into new designs of reactors. Nevertheless, the ability of the community to utilize these immense efforts is very much limited due to the fact that there are hardly any tools that enable the reader to compare between different sets of experiments done by different groups around the globe. Moreover, in many cases the kinetic data is published without mentioning the photocatalyst's irradiated area, thus preventing any comparison. Recent years have witnessed the development of models that facilitate some comparison between experiments that were carried out in reactors of different configurations. This includes also the developing of evaluation tools based on energy considerations, such as the photocatalytic thermodynamic efficiency factor (PTEF) (Serrano and de Lasa, 1997) used in water treatment. Nevertheless, this is not enough. There should be ways to facilitate a simple comparison between catalysts and reactor configurations. An intensive effort in the direction of standardization is taking place these days, initiated by Japan and the European Community. It is hoped that this effort will be materialized, as this may have a huge impact toward successful products.

7.4. Deactivation

The problem of deactivation was known to most of the researchers in the community for many years, as discussed above. Over the years, some means to fight this phenomenon have been proposed (Alberici and Jardim, 1997; Ameen and Raupp, 1999; Cao et al., 2000). Yet, research, focusing on trying to solve this problematic issue, is quite scarce. Whenever deactivation and regeneration are mentioned, they always appear as an unintended spin-off of the research. To the best of our knowledge and understanding, for this reason there are in the market quite a few products that might not meet the life span declared by the manufacturer. Our feeling is that deactivation is not just an issue for manufacturers to take care of, as it may require extensive basic research.

8. CONCLUDING REMARKS

This chapter tried to summarize a few of the aspects related to photocatalytic air treatment. Particular efforts were made to identify the large variety of photocatalytic reactors for indoor air treatment and to point toward the prospects and obstacles in utilizing titanium dioxide for this purpose.

In a manuscript published in 1997, Gregory Raupp has stated that "although it is relatively straightforward to design a laboratory scale reactor that simultaneously contacts a uniformly irradiated catalyst and air effectively, the issues of UV distribution and utilization (energy cost) make reactor design a difficult problem at the commercial level" (Raupp et al., 1997). It seems that the statement made by Raupp et al. in 1997 is still valid and will continue to inspire researchers in their continuing efforts. That way or another, what comes clear from this review is that there cannot be one single solution to be crowned as the ultimate photocatalytic reactor design.

Nevertheless, the increasing number of patents and, more important, the increasing number of products in the market send a clear message that although this aim was not achieved yet, it is not beyond the abilities of science.

ACKNOWLEDGMENT

The assistance of Mr. Yuval Gamliel in the literature search and in drawing the figures is gratefully acknowledged.

LIST OF SYMBOLS

Latin letters

a_V	The total effective catalyst area per unit volume of the reactor ($m^2\,m^{-3}$)
C	Bulk gas-phase concentration
C_A	The concentration of pollutant A

C_{A0} The initial concentration of pollutant A
C_{in} The concentration of pollutant at the reactor's inlet
C_{out} The concentration of pollutant at the reactor's outlet
C_s The mean concentration at the external surface
Cs Concentration at the surface of the photocatalyst
D The diffusion coefficient of the pollutant in air
k True rate constant in LH expression (mol L^{-1} min^{-1})
k^* Apparent rate constant in LH expression
K The Langmuir adsorption constant (L mol^{-1})
L The reactor length
u The flow velocity
Z Axial position along the reactor
K_A The adsorption coefficient of A
k_m The mass transfer coefficient from the gas to catalyst surface (m min^{-1})
$k_{r,A}$ The reaction rate constant
L The characteristic length of the porous photocatalyst
m Meter
r_A The disappearance of A
r_{A0} The initial disappearance of A
r_v The experimental mean rate of reaction per unit volume of catalyst
s Second
t Time
y_i Represents the molar ration of component i

Greek letters

ε The catalyst "grain" porosity
θ_A The surface coverage of this specie
τ The pore skewness

ABBREVIATIONS

AC Activated carbon
A&S Adsorb and Shuttle
AOP Advanced oxidation processes
APQ Apparent quantum efficiency
app. Approximately
BTEX An acronym for a group of aromatic compounds consisting of benzene, toluene, ethylbenzene, and xylenes
CFD Computational fluid dynamics
CSTR Continuous stirred tank reactor
DCA Dichloroacetaldehyde (CCl_2HCOH)
DCAA Dichloroacetic acid (CCl_2HCOOH)

DCAC	Dichloroacetyl chloride ($CHCl_2COCl$)
EPA	Environmental Protection Agency
AQY	Apparent quantum yield
FBR	Fluidized bed reactor
FT-IR	Fourier-transformed infra red spectroscopy
GC-FID	Gas chromatograph, flame ionization detector
GC-MS	Gas chromatograph, mass spectroscopy
HAD	Hexadecylamine
LH	Langmuir–Hinshelwood kinetics expression
MTBE	methyl tert-butyl ether
NO_X	Nitrogen oxides
OQY	Overall quantum yield
OSHA	The Occupational and Safety Administration (US)
PBR	Packed bed reactor
PCE	Perchloroethylene
PFR	Plug flow reactor
ppb	Parts per billion (usually by volume)
ppmv	Parts per million by volume
PQY	Primary quantum yield
PTEF	Photocatalytic thermodynamic efficiency factor
RH	Relative humidity
SBS	Sick building syndrome
TCD	Thermal conductive detector
TCE	Trichloroethylene
TCP	trichloropropene
UV	Ultraviolet
VOCs	Volatile organic compounds
W	Watt

REFERENCES

Agrios, A.G., and Pichat, P. *J. Appl. Electrochem.* **35**, 655 (2005).

Aguado, S., Polo, A., Bernal, M., Coronas, J., and Santamaria, J. *J. Membrane Sci.* **240**, 159 (2004).

Alberici, R.M., and Jardim, W.F. *Appl. Catal. B* **14**, 55 (1997).

Ameen, M.M., and Raupp, G.B. *J. Catal* **184**, 112 (1999).

Ao, C.H., and Lee, S.C. *Chem. Eng. Sci.* **60**, 103 (2005).

Ao, C.H., and Lee, S.C. *J. Photochem. Photobiol. A Chem.* **161**, 131 (2004).

Arabatzis, I.M., and Falara, P. *Nanoletters* **3**, 249 (2003).

Arabatzis, I.M., Spyrellis, N., Loizos, Z., and Falaras, P. *J. Mater. Process. Technol.* **161**, 224 (2005).

Araña, J., Peña Alonso, A., Doña Rodriguez, J.M., Herrera Melian, J.A., Gonzales Diaz, O., and Perez Peña, J. *Appl. Catal. B* **78**, 355 (2008).

Blanco, J., Avila, P., Bahamonde, A., Alvarez, E., Sanchez, B., and Romero, M. *Catal. Today* **29**, 437 (1996).

Blount, M.C., and Falconer, J.L. *J. Catal.* **200**, 21 (2001).

Bolton, J.R., Safarzadeh-amiri, A., and Cater, S.R. The detoxification of waste water streams using solar and artificial UV light sources. *in* F.S. Sterret (Ed.), "Alternative Fuels and the Environment". Lewish Publishers, Boca Raton, FL (1995), p. 187.
Boulamanti, A.K., and Philippopoulos, C.J. *J. Hazard. Mater.* **160**, 83 (2008).
Bouzaza, A., and Laplanche, A. *J. Photochem. Photobiol. A Chem.* **150**, 207 (2002).
Bouzaza, A., Vallet, C., and Laplanche, A. *J. Photochem. Photobiol. A Chem.* **177**, 212 (2006).
Box, G.E.P., and Draper, N.R. *Biometrica* **52**, 355 (1965).
Cao, L.X., Gao, Z., Suib, S.L., Obee, T.N., Hay, S.O., and Freihaut, J.D. *J. Catal*. **196**, 253 (2000).
Cassano, A., Martin, C., Brandi, R., and Alfano, O. *Ind. Eng. Chem. Res.* **34**, 2155 (1995).
Chin, P., Yang, L.P., and Ollis, D.F. *J. Catal.* **237**, 29 (2006).
Cunningham, J., Tobin, J.P.J., and Meriaudeau, P. *Surf. Sci.* **108**, L465 (1981).
de Lasa, H., and Ibrahim, H.U.S. Patent, 6,752,957 (2004).
de Lasa, H., Serrano, B., and Salaices, M. "Photocatalytic Reaction Engineering". Springer, New York (2005).
Destaillats, H., Maddalena, R.L., Singer, B.C., Hodgson, A.T., and McKone, T.E. *Atmos. Environ.* **42**, 1371 (2008).
d'Hennezel, O., and Ollis, D.F. *J Catal* **167**, 118 (1997).
d'Hennezel, O., Pichat, P., and Ollis, D.F. *J. Photochem. Photobiol. A* **118**, 197 (1998).
Dibble, L.A., and Raupp, G.B. *Catal. Lett.* **4**, 345 (1990).
Dibble, L.A., and Raupp, G.B. *Environ. Sci. Technol.* **26**, 492 (1992).
Doucet, N., Bocquillon, F., Zahraa, O., and Bouchy, M. *Chemosphere*, **65**, 1188 (2006).
Driessen, M.D., Goodman, A.L., Miller, T.M., Zaharias, G.A., and Grassian, V.H. *J. Phys. Chem. B* **102**, 549 (1998).
Environmental Protection Agency (EPA). "Total Exposure Assessment Methodology(TEAM) study". Report 600/6-87/002a, Washington, DC (1987).
Fan, J., and Yates, Jr. J.T. *J. Am. Chem. Soc.* **118**, 4686 (1996).
Formenti, M., Juillet, F., Meriaudeau, P., and Teichner, S. *Chem. Technol.* **1**, 680 (1971).
Fox, M.A., and Dulay, M.T. *Chem Rev.* **93**, 341 (1993).
Fujishima, A., Hashimoto, K., Watanabe, T., "TiO_2 Photocatalysis: Fundamentals and Applications". BKC Inc., Tokyo (1999), p. 59.
Fujishima, A., and Honda, K. *Nature* **238**, 37 (1972).
Furman, M., Corbel, S., Le Gall, H., Zahraa, O., and Bouchy, M. *Chem. Eng. Sci.* **62**, 5312 (2007).
Ghosh-Mukerji, S., Haick, H., and Paz, Y. *J. Photochem. Photobiol*. **160**, 77 (2003).
Goswami, D.Y., Trivedi D.M., and Block, S.S. *J. Solar Energy Eng.* **119**, 92 (1997).
Haick, H., and Paz, Y. *J. Phys. Chem. B* **105**, 3045 (2001).
Hashimoto, K., Wasada, K., Toukai, N., Kominami, H., and Kera, Y. *J. Photochem. Photobiol. A Chem.* **136**, 103 (2000).
Hill, C.G. "An Introduction to Chemical Engineering Kinetics & Reactor Design". John Wiley & Sons, NY (1977), p. 429.
Hwang, S.-J., Petucci, C., and Raftery, D. *J. Am. Chem. Soc.* **120**, 4388 (1998).
Ibhadon, A.O., Arabatzis, I.M., Falaras, P., and Tsoukleris, D. *Chem. Eng. J.* **133**, 317 (2007).
Ibrahim, H., and de Lasa, H. *AIChE J.* **50**, 1017 (2004).
Ibrahim, H., and de Lasa, H. *Appl. Catal.* **38**, 201 (2002).
Ibrahim, H., and de Lasa, H. *Chem. Eng. Sci.* **58**, 943 (2003).
Ibsuki, T., and Takeuchi, K. *Atmos. Environ.* **20**, 1711 (1986).
Imoberdorf, G.E., Irazoqui, H.A., Alfano, O.M., and Cassano, A.E. *Chem. Eng. Sci.* **62**, 793 (2007).
Jacoby, W.A., Nimlos, M.R., Blake, D.M., Noble, R.D., and Koval, C.A. *Environ. Sci. Technol.* **28**, 1661 (1994).
Junio, C.T., and Raupp, G.B. *Appl. Surf. Sci.* **72**, 321 (1993).
Kachina, A., Preis, S., and Kallas, J. *Int. J. Photoenergy* **2**, 79847/1 (2007).
Kim, J.S., Itoh, K., Murabayashi, M., and Kim B.A. *Chemosphere* **38**, 2969 (1999a).
Kim, H.H., Tsunoda, K., Katsura, S., and Mizuno, A. *IEEE Trans. Ind. Appl.* **35**, 1306 (1999b).

Kitano, M, Matsuoka, M, Ueshima, M., and Anpo, M. *Appl. Catal. A Gen.* **325**, 1 (2007).
Ku, Y., Ma, C.-M., and Shen, Y.-S. *Appl. Catal. B Environ.* **34**, 181 (2001).
Larson, S.A., and Falconer, J.L. *Catal. Lett.* **44**, 57 (1997).
Larson, S.A., and Falconer, J.L. Characterization of TiO2 Used in Liquid Phase and Gas Phase Photooxidation of Trichloroethylene. *in* D.F. Ollis, and H. Al-Ekabi (Eds.), "Photocatalytic Purification of and Treatment of Water and Air". Elsevier Science Publishers, Amsterdam (1993), p. 473.
Lee, M.C, and Choi, W. *J. Phys. Chem. B* **106**, 11818 (2002).
Lee, S.C., Lam, S., and Fai, H.K. *Build. Environ.* **36**, 837 (2001).
Levenspiel, O. Solid Catalysed Reactions. in "Chemical Reaction Engineering, 3rd Edn.". John Wiley & Sons, New York (1998), p. 388.
Lewandowski, M., and Ollis, D.F. Photocatalytic Oxidation of Gas- Phase Aromatic Contaminants. in V. Ramamurthy, and K.S. Schanze (Eds.), "Semiconductor Photochemistry and Photophysics". Marcel Dekker, New York (2003), p. 249.
Lichtin, N.N., Avudaithai, M., Berman, E., and Dong, J. *Res. Chem. Intermed.* **20**, 755 (1994).
Lim, T.H., Jeong, S.M., Kim, S.D., and Gyenis, J. *J. Photochem. Photobiol. A Chem.* **134**, 209 (2000).
Lim, T.H., and Kim, S.D. *Chemospere* **54**, 305 (2004).
Lin, H.F., Ravikrishna, R., Valsaraj, K.T., *Sep. Purif. Technol.* **28**, 87 (2002).
Luo, Y., and Ollis, D.F. *J. Catal.* **163**, 1 (1996).
Maggos, Th., Plassais, A., Bartzis, J.G., Vasilakos, Ch., Moussiopoulos, N., and Bonafous, L. *Environ. Monit. Assess.* **136**, 35 (2008).
Martra, G, Coluccia, S., Marchese, L., Auguliaro, V., Loddo, V., Palmisano, L., and Schiavello, M. *Catal. Today* **53**, 695 (1999).
Matsuda, S., and Hatano, H. *Powder Technol.* **151**, 61 (2005).
Mehrvar, M., Anderson, W.A., Moo-Young, M., and Reilly, P.M. *Chem. Eng. Sci.* **55**, 4885 (2000).
Mendez-Roman, R., and Cardona-Martinez, N. *Catal. Today* **40**, 353 (1998).
Mills, A., and Le Hunte, S. *J. Photochem. Photobiol. A Chem.* **108**, 1 (1997).
Mohseni, G.M., and Taghipour, F. *Chem. Eng. Sci.* **59**, 1601 (2004).
Monteagudo, J.M., and Duran, A. *Chemosphere* **65**, 1242, (2006).
Muggli, D.S., and Falconer, J.L. *J. Catal.* **175**, 213 (1998).
Muggli, D.S., Lowery, K.H., and Falconer, J.L. *J. Catal.* **180**, 111 (1998).
Murakami, Y., Endo, K., Ohta, I., Nosaka, A.Y., and Nosaka, Y. *J. Phys. Chem. C* **111**, 11339 (2007).
Nicolella C., and Rovatti M. *Chem. Eng. J.* **69**, 119 (1998).
Nimlos, M.R., Jacoby, W.A., Blake, D.M., and Milne, T.A. *Environ. Sci. Technol.* **27**, 732 (1993).
Obee, T.N., and Brown, R.T. *Environ. Sci. Technol.* **29**, 1223 (1995).
Oda, T., Yamashita, R., Haga, I., Takahushi, T., and Masuda, S. *J. Electrostat.* **57**, 293 (2003).
Oda, T., Yamashita, R., Takahushi, T., and Masuda, S. *IEEE Trans. Ind. Appl.* **32**, 118 (1996).
Ollis, D.F., Pelizzetti, E., and Serpone, N. *Environ. Sci. Technol.* **25**, 1523 (1991).
Paz, Y. *Comptes Rendus Chimie* **9**, 774 (2006).
Paz, Y. "Composite Titanium Dioxide Photocatalysts and the "Adsorb & Shuttle" Approach: A review", in "*Solid- State Chemistry and Photocatalysis of Titanium Dioxide*". Nowotny J. (Editor), Trans Tech Publications, UK [in press].
Paz, Y., and Heller, A. *J. Mater. Res.* **12**, 2759 (1997).
Paz, Y., Luo, Z., Rabenberg, L., and Heller, A. *J. Mater. Res.* **10**, 2842 (1995).
Peill, N., and Hoffmann, M. *Environ. Sci. Technol.* **29**, 2974 (1995).
Pelizzetti, E., Visca, M., Borgarello, E., Pramauro, E., and Palmas, A. *Chimica e l'Industria* **63**, 805 (1981).
Peral, J., and Ollis, D.F. *J. Catal.* **136**, 554 (1992).
Phillips, L.A., and Raupp, G.B. *J. Mol. Catal.* **77**, 297 (1992).
Pruden, A.L, and Ollis, D.F. *J. Catal.* **82**, 404, (1983).
Raupp, G.R., Nico, J.A., Annangi, S., Changrani, R., and Annapragada, R. *AIChE J.* **43**, 792 (1997).

Roland, U., Holzer, F., and Kopinke, F.-D. *Catal. Today* **73**, 315 (2002).
Romero-Vargas Castrillon, S., and De-Lasa, H.I. *Ind. Eng. Chem. Res.* **46**, 5867 (2007).
Romero-Vargas Castrillon, S., Ibrahim, H., and De-Lasa, H.I. *Chem. Eng. Sci.* **61**, 3343 (2006).
Saarela, K., Tirkkonen, T., Laine-Ylijoki, J., Jurvelin, M.J., Nieuwenhuijsen, M.J., and Jantunen, M. *Atmos. Environ*. **37**, 5563 (2003).
Sagatelian, Y., Sharabi, D., and Paz, Y. *J. Photochem. Photobiol. A* **174**, 253 (2005).
Salvado-Estivill, I., Brucato, A., and Li Puma, G. *Ind. Eng. Chem. Res*. **46**, 7489 (2007a).
Salvado-Estivill, I., Hargreaves, D.M., and Li Puma, G. *Environ. Sci. Technol.* **41**, 2028 (2007b).
Sampath, S., Uchida, H., and Yoneyama, H. *J. Catal.* **149**, 189 (1994).
Sanhueza, E., Hisatsune, I.C., and Heicklen, J. *Chem. Rev.* **76**, 801 (1976).
Sauer, M.L., Hale, M.A., and Ollis, D.F. *J. Photochem. Photobiol. A* **88**, 169 (1995).
Sauer, M.L., and Ollis, D.F. *J. Catal*. **149**, 81 (1994).
Sclafani, A., Brucato, A., and Rizzuti, L. Mass transfer limitations in a packed bed photoreactor used for phenol removal. in D.F. Ollis, H. Al-Ekabi (Eds.), "Photocatalytic Purification and Treatment of Water and Air", vol. 3. Elsevier, (1993), p. 511.
Serrano, B., and de Lasa, H. *Ind. Chem. Eng. Res*. **36**, 4705 (1997).
Sharabi, D., "Preferential Photodegradation of Contaminants by Molecular Imprinting on a Photocatalytic Substrate" Msc. thesis, Technion, Israel (2007).
Shiraishi, F., Yamaguchi, S., and Ohbuuchi, Y. *Chem. Eng. Sci*. **58**, 929 (2003).
Sidheswaran, M., and Taviarides, L.L. *Ind. Eng. Chem. Res*. **47**, 3346 (2008).
Stokke, J.M., Mazyck, D.W., Wu, C.Y., and Sheahan, R. *Environ. Prog*. **25**, 312 (2006).
Strini, A., Cassese, S., and Schiavi, L. *Appl. Catal. B Environ.* **61**, 90 (2005).
Sun, R.-B., Xi, Z.-G., Chao, F.-H., Zhang, W., Zhang, H.-S., and Yang, D.-F. *Atmos. Environ.* **41**, 6853 (2007).
Takeuchi, K. *J. Jpn. Soc. Atmos. Environ*. **33**, 139 (1998).
Tatsuma, T., Tachibana, S., and Fujishima, A. *J. Phys. Chem. B* **105**, 6987 (2001).
Thevenet, F., Guaiella, O., Puzenat, E., Herrmann, J.-M., Rousseau, A., and Guillard, C. *Catal. Today* **122**, 186 (2007).
Torimoto, T., Okawa, Y., Takeda, N., and Yoneyama, H. *J. Photocem. Photobiol. A Chem.* **103**, 153 (1997).
Tsoukleris, D.S., Maggos, T., Vassilakos, C., and Falaras, P. *Catal. Today* **129**, 96 (2007).
Tsuru, T., Kan-no, T., Yoshioka, T., and Asaeda, M. *J. Memb. Sci.* **280**, 156 (2006).
Turchi, C.S., and Ollis, D.F. *J. Catal.* **122**, 178 (1990).
Upadhya, S., and Ollis, D.F. *J. Adv. Oxid. Technol.* **3**, 199 (1998).
Vorontsov, A.V., and Dubovitskaya, V.P. *J. Catal.* **221**, 102 (2004).
Vorontsov, A.V., Savinov, E.N., Barannik, G.B., Troitsky, V.N., and Parmon, V.N., *Catal. Today* **39**, 207 (1997).
Wang, C.-Y., Rabani, J., Bahnemann, D.W., and Dohrmann, J.K. *J. Photochem. Photobiol. A Chem.* **148**, 169 (2002).
Yamazaki–Nishida, S., Fu, X., Anderson, M.A., and Hori, K. *J. Photochem. Photobiol. A Chem.* **97**, 175 (1996).
Yamazaki-Nishida, S., Nagano, K.J., Phillips, L.A., Cervera-March, S., and Anderson, M.A. *J. Photochem. Photobiol. A Chem.* **70**, 95 (1993).
Yin, S., Liu, B., Zhang, P., Morikawa, T., Yamanaka, K.-I., and Sato, T. *J. Phys. Chem. C* **112**, 12425 (2008).
Yoneyama, H., and Torimoto, T. *Catal. Today* **58**, 133 (2000).
Zemel, E., Haick, H., and Paz, Y. *J. Adv. Oxid. Technol*. **5**, 27 (2002).
Zhou, L., Tan, X., Zhao, L., and Sun, M. *Korean J. Chem. Eng.* 24, 1017 (2007).